Fizika Nizkikh Temperatur, 1997, v. 23, № 3, c. 249–270

Scattering theory of superconductive tunneling in quantum junctions

V. S. Shumeiko[1,2], E. N. Bratus'[1,2], and G. Wendin[1]

[1] *Department of Applied Physics, Chalmers University of Technology and Göteborg University, S-41296 Göteborg, Sweden*

[2] *B. Verkin Institute for Low Temperature Physics and Engineering, 47 Lenin Ave., 310164 Kharkov, Ukraine*

Submitted September 11, 1996, revised September 27, 1996

A consistent theory of superconductive tunneling in single-mode junctions within a scattering formulation of Bogolyubov-de Gennes quantum mechanics is presented. The dc Josephson effect and the dc quasiparticle transport in the voltage-biased junctions are considered. Elastic quasiparticle scattering by the junction determines the equilibrium Josephson current. The origin of Andreev bound states in tunnel junctions and their role in equilibrium Josephson transport are discussed. In contrast, quasiparticle tunneling in voltage-biased junctions is determined by inelastic scattering. A general expression for inelastic scattering amplitudes is derived and the quasiparticle current is calculated at all voltages with emphasis on a discussion of the properties of subgap tunnel current and the nature of subharmonic gap structure.

PACS: 74.50.+r, 74.20. Fg, 74.80. Fp

1. Introduction

The tunnel Hamiltonian model [1] has for many years been a main theoretical tool for investigation of tunneling phenomena in superconductors [2]. However, interpretation of recent experiments on transmissive tunnel junctions [3–5] and complex superconductor-semiconductor structures [6,7] requires more detailed knowledge of the mechanisms of the superconductive tunneling than the tunnel model is able to provide. Particularly informative are experiments on superconducting quantum point contacts with controlled number of transport modes and transparency, such as controllable superconducting break junctions [8] and gate-controlled superconductor–semiconductor devices [9]. Since only a few transport modes with controlled transparency are involved in the tunnel transport, the experiments provide precise and detailed information which can be directly compared with theory.

The first attempts to develop a theory of superconductive tunneling beyond the tunnel Hamiltonian model [10–13] were made in generalization of methods applied to *SNS* junctions [14,15] and superconducting constrictions [16,17] based on the Green's function methods. In these theories, the junction Green's functions are directly found from the Green's function equations which are supplemented by special boundary conditions representing the tunnel barrier or by matching the superconductor and insulator Green's functions at the superconductor-insulator boundaries.

In the first studies of the Josephson effect in *SNS* junctions [18,19] another method of calculation, based on expansion over eigenstates of the Bogolyubov-de Gennes (BdG) equation, has been used [20]. A similar method has been also applied to *SIS* tunnel junctions [21] and superconductor–semiconductor junctions [22]. In the absence of inelastic scattering the method of using the BdG equation gives the same results as the Green's function method [21]. One might then expect that the Josephson effects in superconducting junctions can be explained on a rather simple quantum-mechanical level. Following this idea, the quantum-mechanical approach has been successfully applied to calculation of the direct Josephson current in different kinds of mesoscopic weak links [24–28] and tunnel junctions [29–31]. This method was applied for the first time to voltage-biased junctions by Blonder, Tinkham, and Klapwijk, who considered quasiparticle tunneling in *SIN* junctions as a scattering problem in BdG quantum mechanics [23]. Later, the quantum-mechanical approach has been found helpful in investigations of more complex phenomena of quasiparticle transport and ac Josephson effect in voltage-biased *SNS* junctions [32], mesoscopic *SIS* tunnel junctions [33] and mesoscopic constrictions [34].

The quantum-mechanical approach based on the BdG equation is adequate for describing the physical

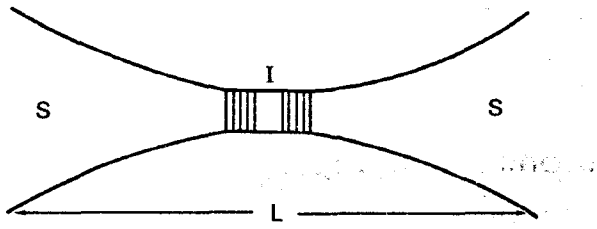

Fig. 1. SIS tunnel constriction.

situation in mesoscopic junctions, where the inelastic scattering effects are weak and most important is the coherent electron dynamics. Because of the quantization of transverse electron modes in mesoscopic junctions [24,35], $1D$ models for the current transport through the junction may be appropriate.

In this paper we present a consistent quantum-mechanical theory of superconductive tunneling in a one–mode quantum constriction (Fig. 1). We consider the dc Josephson effect and also dc quasiparticle tunneling in the voltage-biased junctions. In the latter case we focus attention on a detailed calculation of the subharmonic gap structure (SGS) of the tunnel current [33].

Following the Landauer approach [36], we consider superconducting electrodes as equilibrium reservoirs which emit quasiparticles into the constriction. Scattering by the junction goes into two channels: (i) the normal channel in which the outgoing quasiparticles remain in the same branch of the quasiparticle spectrum, and (ii) the Andreev channel in which quasiparticles change branch due to electron-hole conversions. The current in such a picture results from the imbalance of currents carried by scattering states originating from the left and the right reservoirs. Here the magnitude of the current is proportional to the transmission coefficient D of the tunnel barrier.

The imbalance of currents in superconducting junctions can be created in two ways: by establishing a difference in the phases of the order parameters in the left and right electrodes or by applying a voltage bias. The basic fact concerning the flow of equilibrium current in the presence of a phase difference, which was established by Furusaki and Tsukada [29], is that a bulk supercurrent is, upon approaching the tunnel interface, transformed into a current that flows through the superconducting bound states which appear at the tunnel interface in the presence of the phase difference [37] and which provide transmission of the Cooper pairs through the tunnel barrier. The balance among currents of different scattering states is not violated, although the scattering amplitudes depend strongly on the phase difference.

Application of a voltage bias gives rise to more far-reaching consequences than just the imbalance of the elastic scattering modes: the scattering states themselves are modified in a nontrivial way. This follows from the fact that the scattering amplitudes, which are phase-dependent at equilibrium, become time-dependent in accordance with the Josephson relation [38], $d\varphi/dt = 2eV$, when voltage is applied. Thus, in the presence of a constant voltage the superconducting junction behaves as an effective nonstationary scatterer, whose transmissivity oscillates. This property of the superconducting junctions gives rise to ac Josephson effect; however, it is also significant for dc quasiparticle transport, because the quasiparticle transmission through such a scatterer is *inelastic*.

The physical mechanism of inelastic quasiparticle transmission through voltage-biased superconducting junctions has been first considered in *SNS* junctions [32], where it has been explained in terms of multiple Andreev reflections (MAR): the normal quasiparticles, which are confined between superconducting walls, are permanently accelerated by the static electric field due to sequential electron-hole conversions at the *NS* interfaces, similarly to acceleration of the electrons in an ordinary potential well by a time-dependent electric field. Similar arguments can be extended to the tunnel junctions [39]. However, in tunnel junctions the scattering theory approach is more appropriate because of the quantum nature of quasiparticle transmission through the atomic-size tunnel barrier. This introduces a side band spectrum of scattered waves where the side band energies are shifted with respect to the energy of the incident wave by integer number of quanta of the scatterer frequency [33]. Such an approach is familiar in the theory of quantum scattering by oscillating potential barriers in normal tunnel junctions (see, e.g., Refs. 40 and 41 and the references cited there).

The tunneling through all the inelastic channels (normal and Andreev channels) constitutes a complete picture of superconductive tunneling in biased Josephson junctions — the incoherent part of the side band currents, which correspond to the direct quasiparticle current, and the side band interference currents, which correspond to the alternating Josephson current. An important aspect of this picture is that the Andreev bound states are involved in the current transport together with the extended side band states, which give a multiparticle character to the superconductive tunneling in the subgap voltage region. This multiparticle origin of the subgap tunnel current was first pointed out by Schrieffer and Wilkins [42].

The structure of the paper is as follows. After formulation of the problem and discussion of the quasiclassical approximation in Sec. 2, we consider the problem of elastic scattering in Sec. 3 as a starting point for construction of inelastic scattering states in biased junctions. The solution of the elastic scattering problem allows us to calculate the dc Josephson current, which is done for completeness in Sec. 4. In Sec. 5 we construct inelastic scattering states and derive a continued-fraction representation for the scattering amplitudes. In Sec. 6 we derive the nonequilibrium current. In Sec. 7 we discuss the origin of the excess tunnel current in the large bias limit. In Sec. 8 we present a general analysis of the subgap tunnel current. Finally, the *SGS* is analyzed in Sec. 9.

2. Formulation of the model

We consider a superconducting quantum constriction with adiabatic geometry [43]: the cross section varies smoothly with the coordinate x on the scale of the Fermi electron wavelength $1/p_F$, and the size of the cross section is comparable with the Fermi electron wavelength (Fig. 1). The length L of the constriction is assumed to be smaller than the superconducting coherence length ξ_0:

$$1/p_F \ll L \ll \xi_0 . \qquad (2.1)$$

The Hamiltonian of the constriction is assumed to have the form

$$\hat{H} = \left[\frac{\left(\hat{\mathrm{p}} - \sigma_z e \mathrm{A}(\mathrm{r}, t) \right)^2}{2m} + U(\mathrm{r}) - \mu \right] \sigma_z + \left[V(x) + e\varphi(\mathrm{r}, t) \right] \sigma_z + \hat{\Delta}(\mathrm{r}, t) , \qquad (2.2)$$

where $U(\mathrm{r})$ is the potential which confines the electrons within the constriction; $V(x)$ is the potential of the tunnel barrier; $\mathrm{A}(\mathrm{r}, t)$ and $\varphi(\mathrm{r}, t)$ are electromagnetic potentials; $\hat{\Delta}(\mathrm{r}, t)$ is the off-diagonal superconducting order parameter given by the matrix

$$\hat{\Delta} = \begin{pmatrix} 0 & \Delta e^{i\chi/2} \\ \Delta e^{-i\chi/2} & 0 \end{pmatrix} . \qquad (2.3)$$

We assume that the junction is symmetric. The choice of the units corresponds to $c = \hbar = 1$.

It is convenient to eliminate the phase of the superconducting order parameter $\chi(\mathrm{r}, t)$ in Eq. (2.3) by means of a gauge transformation:

$$\exp(i\sigma_z \chi/2)\, \hat{H} \exp(-i\sigma_z \chi/2) \to \hat{H} , \qquad (2.4)$$

which allows us to introduce a gauge-invariant superfluid momentum, $\mathrm{p}_s = \nabla\chi/2 - e\,\mathrm{A}$, and an electric potential $\Phi = \dot{\chi}/2 + e\varphi$.

There are different scales of change of potentials in Eq. (2.2): one is an atomic scale over which the confining potential $U(r_\perp)$ and the potential of the tunnel barrier $V(x)$ change. Other scales are related to the changes in the superconducting order parameter, the electromagnetic field penetration lengths and the length of the contact: all these lengths are large in comparison with the atomic length. It is convenient to separate these two scales by introducing quasiclassical wave functions [44], which vary slowly on an atomic scale, and by including rapidly varying potentials in a boundary condition for quasiclassical wave functions. To this end, we assume that the solution $\Psi(\mathrm{r}, t)$ of the Bogolyubov-de Gennes equation [20]

$$i\dot{\Psi}(t) = \hat{H}\,\Psi(t) , \qquad (2.5)$$

with the Hamiltonian of Eq. (2.2), has a quasiclassical form

$$\Psi(\mathrm{r}, t) = \sum_\beta \psi_\perp(\mathrm{r}_\perp, x) \frac{1}{\sqrt{v}} \exp\left(i\beta \int p\,dx\right) \psi^\beta(x, t) , \qquad (2.6)$$

where $\psi_\perp$ is the normalized wave function of the quantized transverse electron motion with the energy $E_\perp$,

$$\left(\frac{\hat{\mathrm{p}}_\perp}{2m} + V(\mathrm{r}_\perp, x) \right) \psi_\perp = E_\perp(x) \psi_\perp ,$$

$$\psi_\perp(r_\perp = \infty, x) = 0 ,$$

and p is the longitudinal momentum of the quasiclassical electron, $p(x) = [2m(\mu - E_\perp(x))]^{1/2}$; $\beta = \pm$ indicates the direction of the electron motion. We assume that the constriction has only one transport mode; an extension to the case of several unmixed modes consists of additional summation over all transport modes in the equation for the current. The coefficients ψ^β in Eq. (2.6) describe the wave functions which vary slowly in the x direction and which satisfy the reduced BdG equation

$$i\dot{\psi}^\beta_{L,R} = \left(\beta v \hat{p} \sigma_z + \Phi_{L,R} \sigma_z + v p_{sL,R} + \Delta \sigma_x \right) \psi^\beta_{L,R} \qquad (2.7)$$

in the left (L) and the right (R) electrodes; $v = p/m$. The potentials p_s and Φ describe the distributions of the electromagnetic field and supercurrent in the electrodes. In the point contact geometry these quantities are small due to the effect of spreading out of the current [16,45]. We will therefore omit them, $\mathrm{p}_s = \Phi = 0$. For the same reason, deviation of the spatial distribution of the module of the order

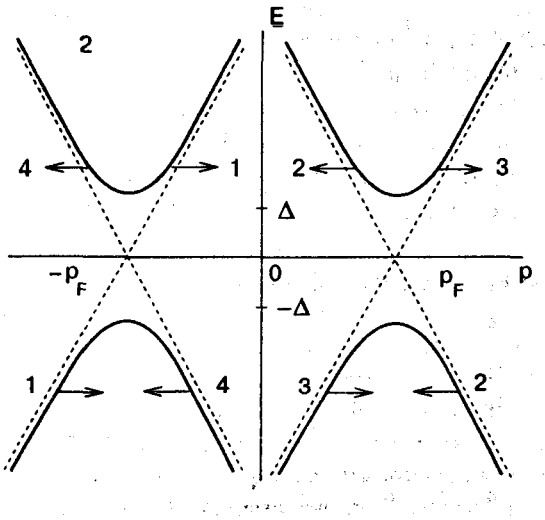

Fig. 2. Quasiparticle spectrum and position of the incoming states: 1(3) — hole (electron)-like quasi-particle incident from left; 2(4) — hole (electron)-like quasiparticle incident from right.

parameter Δ from constant value is small in the point contacts; we will therefore ignore it, $\Delta = \text{const}$.

The functions $\psi^{\beta}_{L,R}$ are matched at the constriction by the boundary condition [31] (see also Appendix A):

$$\begin{pmatrix}\psi^{-}_{L}\\ \psi^{+}_{R}\end{pmatrix} = \hat{V}\begin{pmatrix}\psi^{+}_{L}\\ \psi^{-}_{R}\end{pmatrix} \quad \text{at } x = 0\,, \tag{2.8}$$

with a matching matrix $\hat{V}$

$$\hat{V} = \begin{pmatrix} r & d e^{i\sigma_z \varphi/2} \\ d e^{-i\sigma_z \varphi/2} & r \end{pmatrix}. \tag{2.9}$$

The quantities d and r are the normal electron transmission and reflection amplitudes due to the barrier. Here and further φ is a gauge-invariant difference in the superconducting phases of the right and left electrodes: $\varphi = \chi_R(0) - \chi_L(0)$. The matching matrix in Eq. (2.9) satisfies the unitarity condition

$$\hat{V}\hat{V}^{+} = 1\,. \tag{2.10}$$

The boundary condition in Eqs. (2.8) and (2.9) is analogous to the boundary condition used in the quasiclassical Green's function methods (see, e.g., Refs. 11 and 46). This is a very simple equation for coupling of superconducting electrodes, while retaining the main features of the Josephson effect, except for effects of the resonant tunneling [30, 47, 48].

3. Elastic scattering

In the absence of time dependence in the phase difference at the junction, $\dot{\varphi} = 0$, Eqs. (2.7) and (2.8) describe elastic scattering of quasi-particles. The scattering states can be constructed by using stationary solutions of Eq. (2.7), which correspond to elementary propagating waves with energy $|E| > \Delta$:

$$\psi^{\beta\alpha}_{E} = \exp\left(-iEt + i\beta\alpha(\xi/v)x\right) u^{\delta}_{E}\,, \tag{3.1a}$$

$$u^{\delta}_{E} = (2\cosh\gamma)^{-1/2}\begin{pmatrix} e^{\delta\gamma/2} \\ \sigma e^{-\delta\gamma/2}\end{pmatrix}, \tag{3.1b}$$

where

$$\xi = \sqrt{E^2 - \Delta^2}\,,\ e^{\gamma} = \frac{|E| + \xi}{\Delta}\,,$$

$$\sigma = \text{sign}\, E\,,\ \alpha = \pm\,,\ \text{and}\ \delta = \alpha\sigma\,. \tag{3.2}$$

The vector function u_E is normalized, $(u, u) = 1$; the brackets mean that the scalar product is in the electron-hole space. In Eq. (3.1) there are four elementary waves, which correspond to the same energy, as illustrated in Fig. 2, and which are labeled by quantum numbers β (direction of the Fermi electron momentum) and $\alpha = \text{sign}\,(|p| - p_F)$ (the electron or hole-like branch of the quasiparticle spectrum). The direction of propagation of each elementary wave is determined by the sign of the probability current. The probability current density j_p, which is defined by the conservation law (the continuity equation) $\partial|\psi|^2/\partial t + \partial j_p/\partial x = 0$ for the BdG equation [Eq. (2.7)], has the form $j_p = (\psi, \sigma_z \psi)$. For the elementary waves in Eq. (3.1), we obtain the explicit result $j_p = \beta\delta \tanh\gamma$. According to this formula, the relation $\delta = \beta$ is satisfied for the waves propagating from left to right, and the relation $\delta = -\beta$ is satisfied for the waves propagating from right to left. Therefore, the incoming waves from the left (L) and the right (R) have the form

$$\text{L: } \exp\left(i\sigma(\xi/v)x\right) u^{\beta}_{E}\,, \qquad \text{R: } \exp\left(-i\sigma(\xi/v)x\right) u^{-\beta}_{E}\,, \tag{3.3}$$

while the outgoing waves have the form

$$\text{L: } \exp\left(-i\sigma(\xi/v)x\right) u^{-\beta}_{E}\,,\ \text{R: } \exp\left(i\sigma(\xi/v)x\right) u^{\beta}_{E}\,. \tag{3.4}$$

Correspondingly, the incoming quasiparticle can be scattered into four outgoing states: two forward-scattering states and two backscattering states. One of the reflected waves belongs to the same (electron-like or hole-like) branch of the quasiparticle spectrum as the incoming wave and constitutes the normal scattering channel, while the other reflected wave changes the spectrum branch and constitutes the Andreev channel. In a similar way, transmitted waves constitute normal and Andreev channels. The structure of the scattering states then becomes

$$\begin{pmatrix}\psi_L^- \\ \psi_R^+\end{pmatrix} = \begin{pmatrix}\delta_{j,1} \\ \delta_{j,2}\end{pmatrix} e^{i\sigma(\xi/v)x} u_E^- + \begin{pmatrix}a \\ b\end{pmatrix}_j e^{-i\sigma(\xi/v)x} u_E^+ , \quad (3.5a)$$

$$\begin{pmatrix}\psi_L^+ \\ \psi_R^-\end{pmatrix} = \begin{pmatrix}\delta_{j,3} \\ \delta_{j,4}\end{pmatrix} e^{i\sigma(\xi/v)x} u_E^+ + \begin{pmatrix}c \\ f\end{pmatrix}_j e^{-i\sigma(\xi/v)x} u_E^- , \quad (3.5b)$$

(for brevity we have omitted the time-dependent factors $\exp(-iEt)$). In Eqs. (3.5) the index $j = 1(2)$ corresponds to a hole-like quasiparticle that comes from the left(right), while the index $j = 3(4)$ corresponds to an electron-like quasiparticle that comes from the left (right). According to the structure of the matching matrix [Eq. (2.9)], the symmetry between the scattering states $j = 1$ and 2 is

$$\begin{pmatrix}a \\ b\end{pmatrix}_2 (\varphi) = \begin{pmatrix}b \\ a\end{pmatrix}_1 (-\varphi) , \quad \begin{pmatrix}c \\ f\end{pmatrix}_2 (\varphi) = \begin{pmatrix}f \\ c\end{pmatrix}_1 (-\varphi) . \quad (3.6)$$

Analogous symmetry exists also for the scattering states $j = 3$, 4. Using the unitarity of the matching matrix [Eq. (2.9)], we can find the following relation between the scattering states $j = 3$ and 1:

$$\begin{pmatrix}a \\ b\end{pmatrix}_3 (\gamma, r, d) = \begin{pmatrix}c \\ f\end{pmatrix}_1 (-\gamma, r^*, d^*) ,$$

$$\begin{pmatrix}c \\ f\end{pmatrix}_3 (\gamma, r, d) = \begin{pmatrix}a \\ b\end{pmatrix}_1 (-\gamma, r^*, d^*) . \quad (3.7)$$

These symmetry relations allow us to find all the scattering amplitudes if one of the scattering states is known.

Let us find the explicit scattering amplitudes for the scattering state $j = 1$. After substituting Eqs. (3.5) into Eq. (2.8), it is convenient to split the resulting equation, using the orthogonality condition, $(u^+, \sigma_z u^-) = 0$, into two independent equations for the normal scattering amplitudes c, f and for the Andreev scattering amplitudes a, b:

$$(u^-, \sigma_z u^-)\begin{pmatrix}1 \\ 0\end{pmatrix} = (u^-, \sigma_z \hat{V} u^-)\begin{pmatrix}c \\ f\end{pmatrix}_1 , \quad (3.8a)$$

$$(u^+, \sigma_z u^+)\begin{pmatrix}a \\ b\end{pmatrix}_1 = (u^+, \sigma_z \hat{V} u^-)\begin{pmatrix}c \\ f\end{pmatrix}_1 . \quad (3.8b)$$

Calculating the scalar products in Eqs. (3.8), we find the explicit expression for the Andreev amplitudes in terms of the normal amplitudes,

$$\begin{pmatrix}a \\ b\end{pmatrix}_1 = \frac{id \sin(\varphi/2)}{\sinh\gamma}\begin{pmatrix}f \\ -c\end{pmatrix}_1 . \quad (3.9)$$

The solution of the first equation in Eq. (3.8) is given by

$$c_1 = \frac{r \sinh^2\gamma}{Z} , \quad f_1 = -\frac{d \sinh\gamma \sinh(\gamma + i\varphi/2)}{Z} , \quad (3.10)$$

where

$$Z = -\frac{d}{d^*} \times$$

$$\times \left(R \sinh^2\gamma + D \sinh(\gamma + i\varphi/2) \sinh(\gamma - i\varphi/2)\right) , \quad (3.11)$$

$D = |d|^2$ is the normal electron transmission coefficient of the tunnel junction, and $R = |r|^2 = 1 - D$ is the normal electron reflection coefficient. It follows from Eqs. (3.9) and (3.10) that if there is no phase difference across the junction, $\varphi = 0$, the Andreev scattering channel is closed: $a = b = 0$. It is worth mentioning that the Andreev reflection is also absent if the normal transparency of the junction is equal to zero, $D = 0$. If, on the other hand, the junction is completely transparent for normal electrons, $D = 1$, there is no Andreev forward scattering, $b = c = 0$.

In the presence of a phase difference at the junction the quasiparticle scattering is accompanied by the appearance of superconducting bound states [37]. One can establish the existence of bound states by investigating the poles of the scattering amplitudes, Eq. (3.10), at imaginary γ corresponding to energies lying inside the gap $|E| < \Delta$. Assuming $\gamma \to i\gamma$ in Eq. (3.11), we have the dispersion equation $Z(i\gamma) = 0$ or

$$\sin^2\gamma = D \sin^2\varphi/2 . \quad (3.12)$$

The bound states correspond to a positive value of $\sin\gamma$: $\Delta \sin\gamma = \mathrm{Im}\,\xi > 0$. This condition has two roots:

$$\gamma = \gamma_0 = \arccos(\sqrt{D} \sin\varphi/2) , \quad \gamma = \pi - \gamma_0 \quad (3.13)$$

or

$$E(\varphi) = \pm\Delta\sqrt{1 - D\sin^2\varphi/2} . \quad (3.14)$$

The wave functions of the bound states can be constructed from elementary solutions of Eq. (2.7) with $|E| < \Delta$, which decay at $x = \pm\infty$:

$$\varphi^{\beta}_{E,R} = \exp(-iEt - \zeta x/v)\, u_E^{\nu} , \quad (3.15a)$$

$$\varphi^{\beta}_{E,L} = \exp(-iEt + \zeta x/v)\, u_E^{-\nu} , \quad (3.15b)$$

where

$$u_E^{\nu} = \frac{1}{\sqrt{2}}\begin{pmatrix} e^{i\gamma/2} \\ \sigma e^{-i\gamma/2}\end{pmatrix} , \quad (3.16)$$

$$e^{i\gamma} = \frac{|E| + i\zeta}{\Delta} , \quad \zeta = \sqrt{\Delta^2 - E^2} , \quad \nu = \beta\sigma .$$

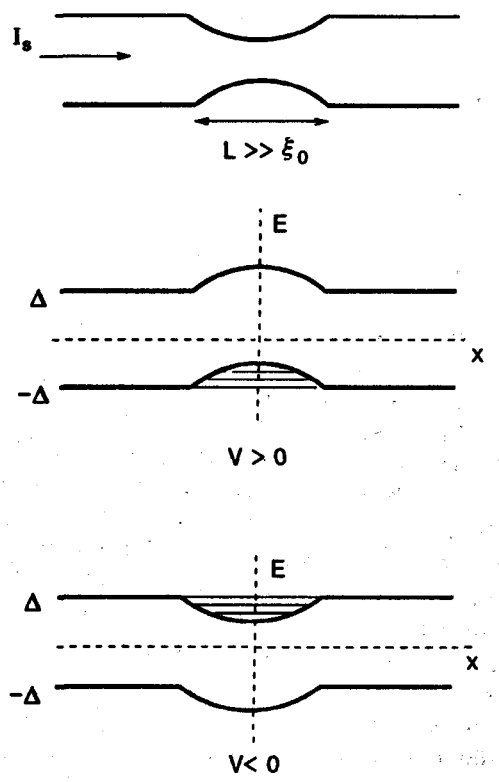

Fig. 3. Spatial configuration of the edges of the superconducting energy bands in a long constriction: E_{min}, $E_{max} = \pm\Delta + p_s(x)v$. A potential well appears in upper (lower) band for electrons moving in a direction opposite to (along) the supercurrent.

The bound state ansatz has a form similar to the outgoing part of the scattering states [Eq. (3.5)] with the coefficients satisfying the homogeneous equations in (3.8). These coefficients are

$$f = -\frac{d \sin(\gamma + \varphi/2)}{r \sin\gamma} c, \qquad (3.17a)$$

$$\begin{pmatrix} a \\ b \end{pmatrix} = \frac{d \sin(\varphi/2)}{\sin\gamma} \begin{pmatrix} f \\ -c \end{pmatrix}, \qquad (3.17b)$$

where γ is given by Eq. (3.12). We note that the bound state spectrum is nondegenerate. The coefficient c in Eqs. (3.17) is obtained from the normalization condition for the bound state wave function,

$$\int d^2 r_\perp \int_{-\infty}^{\infty} dx |\Psi|^2 =$$

$$= \frac{1}{\xi}(|a|^2 + |b|^2 + |c|^2 + |f|^2) = 1,$$

which yields

$$|c|^2 = \Delta \sin\gamma \left(1 + \frac{D}{R} \frac{\sin^2(\gamma + \varphi/2)}{\sin^2\gamma}\right)^{-1} \qquad (3.18)$$

What is the origin of the bound states in a tunnel junction? According to Eq. (3.8), one can regard these states as resulting from hybridization of the bound states in the short ballistic constriction [24] due to the normal electron reflection by the barrier (cf. effect of impurities in the *SNS* junction [25,26]). Let us consider a smooth constriction with the length exceeding the coherence length, $L >> \xi_0$. In such a constriction the supercurrent density and the superfluid momentum are related by the local equation, $J_s(x) = (e/m) N_s p_s(x)$, and they are both enhanced in the neck of the constriction due to current concentration (for simplicity we disregard the effect of suppression of the superfluid electron density N_s by the supercurrent). The local quasiparticle spectrum in the presence of supercurrent has an additional contribution $\pm v_F p_s(x)$ [20], which gives rise to a shift of the local energy gap (Fig. 3). The spatial bending of the gap edges forms the potential wells at $E < 0$ ($E > 0$) for quasiparticles with electron velocities directed along (opposite) the current. The bound states in these potential wells are similar to the Andreev bound states in the *SNS* junctions [49]. The difference is that here the bound states are caused by the spatial inhomogeneity of the *phase* of the order parameter, while the original Andreev states are caused by the spatial inhomogeneity of the modulus of the order parameter. With decreasing length of the constriction, the number of the bound states in the well decreases. The short Josephson constriction corresponds to an infinitely narrow and deep δ-potential well which contains only one Andreev level [24].

4. Direct Josephson current

A convenient expression for the tunnel current results from statistical averaging of the current operator written in the Nambu representation [50]:

$$I(x, t) = \frac{e}{2m} \left\{ (\hat{p} - \hat{p}') \int d^2 r_\perp \times \right.$$
$$\left. \times \left[\delta(\mathbf{r} - \mathbf{r}') \, \mathrm{Tr} \langle \hat{\Psi}(\mathbf{r}, t) \hat{\Psi}^+(\mathbf{r}', t) \rangle \right] \right\}_{\mathbf{r} = \mathbf{r}'}, \qquad (4.1)$$

where $\hat{\Psi}$ is a two-component field operator

$$\hat{\Psi}(\mathbf{r}, t) = \begin{pmatrix} \hat{\psi}_\uparrow(\mathbf{r}, t) \\ \hat{\psi}_\downarrow^+(\mathbf{r}, t) \end{pmatrix}, \qquad (4.2)$$

and Tr is a trace in electron-hole space. The angular brackets in Eq. (4.1) denote a thermal average of the one-particle density matrix of the superconductor [51]. At equilibrium this matrix has the form

$$\langle \hat{\Psi}(\mathrm{r})\,\hat{\Psi}^{+}(\mathrm{r})\rangle = \sum_{\lambda} \Psi_{\lambda}(\mathrm{r}) n_F(-E_{\lambda}) \Psi_{\lambda}^{+}(\mathrm{r}'), \quad (4.3)$$

where $\Psi_\lambda(\mathrm{r})$ are the eigenstates of the steady-state BdG equation [Eq. (2.5)] with the quantum numbers λ. We note that the definition of Fermi distribution function n_F here corresponds to the distribution of holes in the normal metal: in the ground state all energy levels above the Fermi level ($E>0$) are occupied, while energy levels below the Fermi level ($E<0$) are empty (see also the discussion in the next section). In the quasiclassical approximation [Eq. (2.6)] the average tunnel current calculated at the middle of the junction has the form

$$I = -e \sum_{\lambda} n_F(-E_{\lambda}) \sum_{\beta} \beta \left| \psi_{\lambda}^{\beta}(0) \right|^2 . \quad (4.4)$$

The current in Eq. (4.4) can be calculated either at the left or the right side of the junction, because the equality

$$|\psi_L^+|^2 - |\psi_L^-|^2 = |\psi_R^+|^2 - |\psi_R^-|^2 , \quad (4.5)$$

due to the unitarity of the matching matrix $\hat{V}$ in Eq. (2.10), holds for the each eigenstate. The current in Eq. (4.4) consists of contributions from the scattering states and the bound states:

$$I = -\int_{|E|>\Delta} \frac{dE|E|}{2\pi\xi} n_F(-E) \sum_j I_j(E) - \sum_{|E|<\Delta} n_F(-E) I_{\mathrm{bound}}(E), \quad I(E) = e \sum_{\beta} \beta |\psi^{\beta}(E)|^2 . \quad (4.6)$$

When calculating the contribution from the scattering states, it is convenient to consider the transmitted current of each scattering mode:

$$I_j(E) = \begin{cases} e(|b_j|^2 - |f_j|^2) & j = 1, 3, \\ e(|c_j|^2 - |a_j|^2) & j = 2, 4. \end{cases} \quad (4.7)$$

The symmetry relations [Eqs. (3.6) and (3.7)] yield

$$I_1(E) = I_4(E), \; I_2(E) = I_3(E), \; I_2(E) = -I_1(E). \quad (4.8)$$

The currents of all the scattering states with a given energy therefore cancel each other at equilibrium [52]. Substituting Eqs. (3.17) and (3.18) into Eq. (4.6), for, e.g., the right electrode, we obtain the following expression for the current of the bound state:

$$I_{\mathrm{bound}}(E) = e(|b|^2 - |f|^2) = -\frac{e\Delta^2}{2E} D \sin\varphi . \quad (4.9)$$

A useful formula for the current of the single bound state, which allows direct evaluation of the current from the bound state spectrum, is given by equation

$$I(E) = 2e \frac{dE(\varphi)}{d\varphi} , \quad (4.10)$$

where $E(\varphi)$ is the bound state energy band [Eq. (3.14)]. This formula is derived in Appendix B. Taking into account Eqs. (4.9) and (4.6), we write the total current in the form [10–12, 53]

$$I = \frac{e\Delta D \sin\varphi}{2\sqrt{1 - D\sin^2(\varphi/2)}} \tanh \frac{\Delta\sqrt{1 - D\sin^2(\varphi/2)}}{2T} . \quad (4.11)$$

Thus, the Josephson direct current in tunnel junctions is carried only by the bound states, which is similar to the situation found in the other kinds of short weak links [24–26,28,30]. It follows from Eqs. (4.6) and (4.9) that the nonvanishing total current results from the imbalance of the bound state currents due to a difference in the equilibrium population numbers. Creation of a nonequilibrium population makes it possible to control the Josephson transport [28, 31, 48].

5. Inelastic scattering

Let us now discuss inelastic scattering in voltage-biased junctions. According to our assumption $\Phi = 0$, which is explained in Sec. 2, the applied voltage drop V is confined to the constriction; in order not to complicate the problem, we have also disregarded a small time-dependent voltage induced across the junction by the ac Josephson current (self-coupling effect [54]). This implies the following dependence on time of the phase difference:

$$\varphi = \varphi_0 + 2eVt . \quad (5.1)$$

The appearance of factors with periodic time dependence in the boundary condition [Eqs. (2.8) and (2.9)] gives rise to a more complex structure of the scattering states than in Eq. (3.5). In order to satisfy the boundary condition, the outgoing part of the scattering states in Eq. (3.5) is to be constructed from the eigenstates of Eq. (2.7) with different energies $E_n = E - neV$ shifted with respect to the energy E of the incoming wave with an integer $-\infty < n < \infty$ (side band structure)

$$\begin{pmatrix} \psi_L^- \\ \psi_R^+ \end{pmatrix}(0) = \begin{pmatrix} \delta_{j,1} \\ \delta_{j,2} \end{pmatrix} u_E^- e^{-iEt} + \sum_n \begin{pmatrix} a \\ b \end{pmatrix}_{j,n} u_{E_n}^+ e^{-iE_n t} , \quad (5.2a)$$

$$\begin{pmatrix} \psi_L^+ \\ \psi_R^- \end{pmatrix}(0) = \begin{pmatrix} \delta_{j,3} \\ \delta_{j,4} \end{pmatrix} u_E^+ e^{-iEt} + \sum_n \begin{pmatrix} c \\ f \end{pmatrix}_{j,n} u_{E_n}^- e^{-iE_n t} . \quad (5.2b)$$

For brevity we use the notation $u_n = u_{E_n}$. While the incoming state is itinerant, the outgoing states can be either itinerant [Eq. (3.1) if $|E_n| > \Delta$] or bound [Eq. (3.16) if $|E_n| < \Delta$]. It is convenient to combine the two equations for the functions u_n in a single analytical form:

$$u_n^{\pm} = \frac{1}{\sqrt{2\cosh\Gamma_n}} \begin{pmatrix} e^{\pm\gamma_n/2} \\ \sigma_n e^{\mp\gamma_n/2} \end{pmatrix}, \tag{5.3}$$

$$e^{\gamma_n} = \frac{|E_n| + \xi_n}{\Delta}, \quad \Gamma_n = \mathrm{Re}\,\gamma_n,$$

$$\xi_n = \begin{cases} \sqrt{E_n^2 - \Delta^2}, & |E_n| > \Delta, \\ i\sigma_n\sqrt{\Delta^2 - E_n^2}, & |E_n| < \Delta. \end{cases} \tag{5.4}$$

To find the scattering amplitudes in Eq. (5.2) we consider the boundary condition Eq. (2.8). It is important to mention that this boundary condition was derived without regard for the energy dispersion of the normal electron scattering amplitudes d and r, which means that now this assumption should be valid for the entire interval of relevant energies E_n. Let us first discuss $j = 1$ (hole-like quas-particle coming from the left):

$$\begin{pmatrix} 1 \\ 0 \end{pmatrix} u_n^- \delta_{n,0} + \begin{pmatrix} a \\ b \end{pmatrix}_{1,n} u_n^+ =$$

$$= r \begin{pmatrix} c \\ f \end{pmatrix}_{1,n} u_n^- + \frac{d}{2} \begin{pmatrix} 1+\sigma_z & 0 \\ 0 & 1-\sigma_z \end{pmatrix} \begin{pmatrix} f \\ c \end{pmatrix}_{1,n-1} u_{n-1}^- +$$

$$+ \frac{d}{2} \begin{pmatrix} 1-\sigma_z & 0 \\ 0 & 1+\sigma_z \end{pmatrix} \begin{pmatrix} f \\ c \end{pmatrix}_{1,n+1} u_{n+1}^- . \tag{5.5}$$

It is convenient to separate the equations for normal and Andreev scattering amplitudes in Eq. (5.5) using a procedure similar to Eq. (3.8). The equation for the normal scattering amplitudes then becomes

$$rc_{1,n} + (d/2)(V_{nn+1}^- f_{1,n+1} + V_{nn-1}^+ f_{1,n-1}) = \delta_{n0}, \tag{5.6}$$

$$rf_{1,n} + (d/2)(V_{nn+1}^+ c_{1,n+1} + V_{nn-1}^- c_{1,n-1}) = 0,$$

where the coefficients

$$V_{nm}^{\pm} = \frac{(u_n^{-\,*}, \sigma_z \pm 1, u_m^-)}{(u_n^{-\,*}, \sigma_z u_n^-)} \tag{5.7}$$

have the explicit form

$$V_{nm}^+ = -\frac{\exp(-(\gamma_n + \gamma_m)/2)}{\sinh\gamma_n} \left(\frac{\cosh\Gamma_n}{\cosh\Gamma_m}\right)^{1/2}, \tag{5.8a}$$

$$V_{nm}^- = \sigma_n\sigma_m \frac{\exp((\gamma_n + \gamma_m)/2)}{\sinh\gamma_n} \left(\frac{\cosh\Gamma_n}{\cosh\Gamma_m}\right)^{1/2}. \tag{5.8b}$$

The equation for the Andreev scattering amplitudes is

$$a_{1,n} = (d/2)(U_{nn+1}^- f_{1,n+1} + U_{nn-1}^+ f_{1,n-1}^+),$$
$$b_{1,n} = (d/2)(U_{nn+1}^+ c_{1,n+1} + U_{nn-1}^- c_{1,n-1}), \tag{5.9}$$

where the coefficients are defined as

$$U_{nm}^{\pm} = \frac{(u_n^{+\,*}, \sigma_z \pm 1, u_m^-)}{(u_n^{+\,*}, \sigma_z u_n^+)}, \tag{5.10}$$

and have the explicit forms

$$U_{nm}^+ = \frac{\exp((\gamma_n - \gamma_m)/2)}{\sinh\gamma_n} \left(\frac{\cosh\Gamma_n}{\cosh\Gamma_m}\right)^{1/2}, \tag{5.11a}$$

$$U_{nm}^- = -\sigma_n\sigma_m \frac{\exp(-(\gamma_n - \gamma_m)/2)}{\sinh\gamma_n} \left(\frac{\cosh\Gamma_n}{\cosh\Gamma_m}\right)^{1/2}. \tag{5.11b}$$

As can be seen from Eqs. (5.6) and (5.9), the inelastic scattering possesses a specific asymmetry: the forward scattered waves have odd side band indices and backward scattered waves have even side band indices, as illustrated in Fig. 4. Correspondingly, bound states with odd or even side band indices are induced either in the right or in the left electrode. We note that the scattering to any side band consists of normal and Andreev components.

It is instructive to compare the superconducting scattering diagram in Fig. 4 with the scattering diagram of normal junctions. In the normal limit $\Delta = 0$, all the Andreev amplitudes in Eq. (5.9) vanish [$U_n^{\pm} = 0$ in Eq. (5. 11)] and Eq. (5.6) split because $V^+ = 0$ in Eq. (5.8), which yields $f_n = c_{n-1} = 0$ for all $n \neq 1$. Thus, the side band diagram in Fig. 4 reduces to the elementary fragment shown in Fig. 5,*a*. This fragment corresponds to the scattering of a *true hole*, meaning a particle with spectrum $E_h = -(p^2/2m - \mu)$, according to the BdG equations (2.2) and (2.5). In the ground state, $T = 0$, these holes fill all positive energy states $E > 0$, while the negative energy states are empty. For the electrons, the corresponding diagram is sketched in Fig. 5,*b*. In this diagram the chemical potentials in both electrodes are equal, while the energies of the incident and transmitted states are shifted by eV. This difference from the conventional diagram of normal

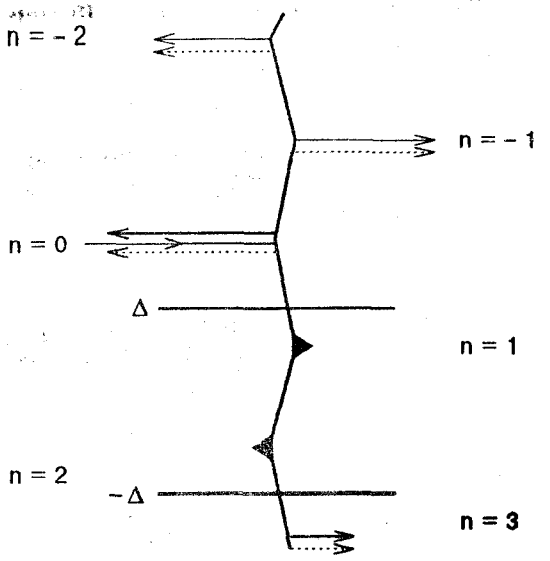

Fig. 4. Scattering diagram of voltage-biased superconducting tunnel junctions. Solid (dotted) arrows indicate scattering in the normal (Andreev) channel. Filled triangles indicate superconducting bound states. Transmission (reflection) occurs into side bands with odd (even) indices.

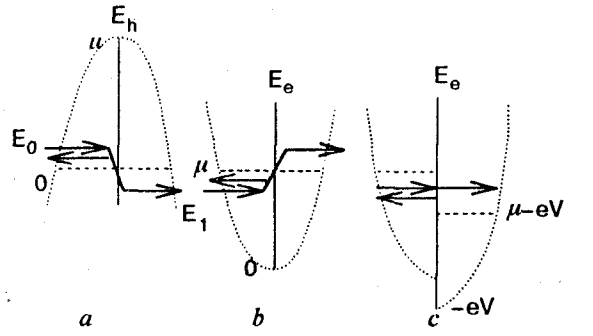

Fig. 5. Scattering diagrams of voltage-biased normal tunnel junctions: scattering of normal holes with spectrum $E_h = \mu - (p^2/2m)$; represents an elementary fragment of the diagram in Fig. 4 for $j = 1$ (*a*); scattering of the normal electrons with spectrum $E_e = p^2/2m$ (*b*); conventional diagram of elastic electron scattering in biased tunnel junctions; the local chemical potentials in the electrodes are then shifted by eV (*c*).

electron tunneling in Fig. 5,*c* (where the chemical potentials in the electrodes are shifted relative to each other, while the scattering is elastic) appears after separating out the superconducting phase in Eq. (2.4); the conventional picture with shifted chemical potential can be restored by means of the gauge transformation of the normal electron wave function $\psi \to \exp(-ieVt)\psi$.

When superconductivity is switched on, $\Delta \neq 0$, the incoming quasi-particle consists of both electron and hole components, and therefore the scattering diagram is a combination of the diagrams in Figs. 5,*a* and 5,*b*. The electron-hole conversion, which leads to the appearance of electron and hole components in the upper and lower transmitted states, must also be taken into account. Continuation of this process creates the whole superconducting scattering diagram in Fig. 4.

From a mathematical point of view, Eqs. (5.6) and (5.9) for the scattering amplitudes are second-order difference equations which cannot be solved exactly, except in special cases, e.g., a fully transparent constriction ($r = 0$), where Eq. (5.6) reduces to a binary relation [34]. In general, it is possible to find asymptotic solutions using a small parameter. In the present case of a tunnel junction, there is a natural small parameter — the transparency of the tunnel barrier: $D \ll 1$. However, a straightforward perturbation expansion with respect to this parameter gives rise to divergences, which are similar to the difficulties encountered in of the multiparticle tunneling theory (MPT) [42,57,58]. In order to formulate an improved perturbation procedure, it is convenient to rewrite Eqs. (5.6) and (5.9) in terms of the parameter $\lambda = D/4R$, the true small parameter of the theory, as will be seen later. Accordingly, we introduce new scattering amplitudes

$$c_{1,\pm 2k} = \frac{\lambda^k}{r} c_{\pm 2k}, \quad f_{1,\pm(2k+1)} = \frac{\lambda^k d^*}{2R} f_{\pm(2k+1)},$$

$$a_{1,\pm 2k} = \lambda^k a_{\pm 2k}, \quad b_{1,\pm(2k+1)} = \frac{\lambda^k d}{2r} b_{\pm(2k+1)}, \quad (5.12)$$

which satisfy equations

$$c_n + \lambda V^-_{nn+1} f_{n+1} + V^+_{nn-1} f_{n-1} = 0,$$

$$f_n - \lambda V^+_{nn+1} c_{n+1} - V^-_{nn-1} c_{n-1} = 0, \quad (5.13a)$$

$$a_n = \lambda U^-_{nn+1} f_{n+1} + U^+_{nn-1} f_{n-1},$$

$$b_n = \lambda U^+_{nn+1} c_{n+1} + U^-_{nn-1} c_{n-1} \quad (5.13b)$$

for $n > 0$. For $n < 0$ it is necessary to make the change $V^{\pm}_{nm} \to V^{\mp}_{-n-m}$, $U^{\pm}_{nm} \to U^{\mp}_{-n-m}$, $(n, m > 0)$ in the above equations. The equation for $n = 0$ can then be written as

$$c_0 + \lambda(V^-_{01} f_1 + V^+_{0-1} f_{-1}) = 1. \quad (5.13c)$$

Let us now turn to the second scattering case in Eq. (5.2), $j = 2$ (hole-like quasi-particle incoming from the right). According to the symmetry relations of Eq. (3.6), the scattering amplitudes $j = 2$ differ from the scattering amplitudes $j = 1$ by $\varphi \to -\varphi$, which in our time-dependent case means that $n \pm 1 \to n \mp 1$. Taking into account this symmetry and also the property of the scattering amplitudes in Eq. (3.6), we introduce new scattering amplitudes

$$f_{2,\pm 2k} = \frac{\lambda^k}{r}\bar{c}_{\pm 2k},$$

$$c_{2,\pm(2k+1)} = \frac{\lambda^k d^*}{2R}\bar{f}_{\pm(2k+1)},\quad b_{2,\pm 2k} = \lambda^k \bar{a}_{\pm 2k}, \tag{5.14}$$

which satisfy the following equations (for $n > 0$):

$$\bar{c}_n + \lambda V^+_{nn+1}\bar{f}_{n+1} + V^-_{nn-1}\bar{f}_{n-1} = 0,$$

$$\bar{f}_n - \lambda V^-_{nn+1}\bar{c}_{n+1} - V^+_{nn-1}\bar{c}_{n-1} = 0, \tag{5.15a}$$

$$\bar{a}_n = \lambda U^+_{nn+1}\bar{f}_{n+1} + U^-_{nn-1}\bar{f}_{n-1},$$

$$\bar{b}_n = \lambda U^-_{nn+1}\bar{c}_{n+1} + U^+_{nn-1}\bar{c}_{n-1}, \tag{5.15b}$$

$$\bar{c}_0 + \lambda(V^+_{01}\bar{f}_1 + V^-_{0-1}\bar{f}_{-1}) = 1. \tag{5.15c}$$

Equations (5.15) differ from Eqs. (5.13) by

$$V^{\pm} \to V^{\mp},\ U^{\pm} \to U^{\mp}. \tag{5.16}$$

In the case of electron-like quasi-particles incoming from the left, $j = 3$, the symmetry of Eq. (3.7) involves transformation $\gamma \to -\gamma$, which means transformation of the coefficients $V^{\pm} \to -\sigma_n\sigma_m V^{\mp}$, $U^{\pm} \to -\sigma_n\sigma_m U^{\mp}$ in Eqs. (5.6) and (5.9). This transformation allows us to relate the scattering amplitudes of this case to the solutions of Eqs. (5.5):

$$a_{3,\pm 2k} = \frac{\lambda^k}{r^*}\sigma_{\pm 2k}\bar{c}_{\pm 2k},$$

$$b_{3,\pm(2k+1)} = -\frac{\lambda^k d}{2R}\sigma_{\pm(2k+1)}\bar{f}_{\pm(2k+1)},$$

$$c_{3,\pm 2k} = \lambda^k \sigma_{\pm 2k}\bar{a}_{\pm 2k}, \tag{5.17}$$

$$f_{3,\pm(2k+1)} = -\frac{\lambda^k d^*}{2r^*}\sigma_{\pm(2k+1)}\bar{b}_{\pm(2k+1)}.$$

In a similar way the scattering amplitudes of electron-like quasi-particles incoming from the right, $j = 4$, are related to the solutions of Eqs. (5.13):

$$b_{4,\pm 2k} = \frac{\lambda^k}{r^*}\sigma_{\pm 2k}\, c_{\pm 2k},$$

$$a_{4,\pm(2k+1)} = -\frac{\lambda^k d}{2R}\sigma_{\pm(2k+1)} f_{\pm(2k+1)},$$

$$f_{4,\pm 2k} = \lambda_k \sigma_{\pm 2k}\, a_{\pm 2k}, \tag{5.18}$$

$$c_{4,\pm(2k+1)} = -\frac{\lambda^k d^*}{2r^*}\sigma_{\pm(2k+1)}\, b_{\pm(2k+1)}.$$

According to the symmetry of the coefficients in Eqs. (5.13) and (5.15),

$$V^{\pm}_{nm}(-E) = V^{\pm\,*}_{-n-m}(E),\ U^{\pm}_{nm}(-E) = U^{\pm\,*}_{-n-m}(E), \tag{5.19}$$

all scattering amplitudes with positive and negative incoming energies are related by the relation

$$a_n(-E) = \bar{a}_{-n}{}^*(E), \tag{5.20}$$

and similarly for the other amplitudes.

Let us now formally solve Eq. (5.13) for $n > 0$ in the form [55]

$$f_{2k+1} = (-1)^k \prod_{l=0}^{2k+1} S_l\, c_o, \tag{5.21}$$

where the quantities S_l are defined as

$$S_{2k} = -\frac{c_{2k}}{f_{2k-1}},\quad S_{2k+1} = \frac{f_{2k+1}}{c_{2k}}, \tag{5.22}$$

and satisfy the recurrence relations

$$S_{2k} = \frac{V^+_{2k,2k-1}}{1 + \lambda V^-_{2k,2k+1}S_{2k+1}},$$

$$S_{2k+1} = \frac{V^-_{2k+1,2k}}{1 + \lambda V^+_{2k+1,2k+2}S_{2k+2}}. \tag{5.23}$$

The quantity c_0 in Eq. (5.27) is given by

$$c_0 = \frac{1}{1 + \lambda(V^-_{01}S_1 + V^+_{0-1}S_{-1})}. \tag{5.24}$$

It is convenient to express the functions S_n in Eq. (5.23) in terms of the relation $S_n = V^{\pm}_{n,n+1}/Z_n$, where the denominators Z_n ($n \neq 0$) satisfy the recurrence relation

$$Z_n = 1 + \lambda\frac{a^{\pm}_n a^{\pm}_{n+1}}{Z_{n+1}},\quad a^{\pm}_n = \frac{e^{\pm\gamma_n}}{\sinh\gamma_n}, \tag{5.25}$$

($\pm$ corresponds to even/odd n), and to define Z_0 as the denominator of c_0, Eq. (5.24):

$$Z_0 = 1 + \lambda\frac{a^+_0 a^+_1}{Z_1} + \lambda\frac{a^-_0 a^-_{-1}}{Z_{-1}}. \tag{5.26}$$

Using the above notation, we can express the coefficients of the normal forward scattering, $|f_n|^2$, in the form

$$|f_n|^2 = \frac{e^{\gamma_0}}{\cosh\gamma_0|Z_0|^2} e^{\Gamma_n} \cosh\Gamma_n \prod_{l=1}^{n} \frac{1}{|Z_l \sinh\gamma_l|^2}. \quad (5.27)$$

The equation for the coefficients of the normal backward scattering, $|c_n|^2$, differs from Eq. (5.27) by $\exp(\Gamma_n) \to \exp(-\Gamma_n)$. The relation between the amplitudes of the Andreev and normal forward scattering in Eq. (5.13) taking into account Eqs. (5.22), (5.23), and (5.25), has the form

$$b_n = -e^{-\gamma_n}\left(1 - \lambda \frac{2e^{-\gamma_{n+1}}}{\sinh\gamma_{n+1} Z_{n+1}}\right) f_n. \quad (5.28)$$

In a similar way, one can express the solution of Eq. (5.15) for $n > 0$ in the form

$$|\bar{f}_n|^2 = \frac{e^{-\gamma_0}}{\cosh\gamma_0|\bar{Z}_0|^2} e^{-\Gamma_n} \times$$

$$\times \cosh\Gamma_n \prod_{l=1}^{n} \frac{1}{|\bar{Z}_l \sinh\gamma_l|^2},$$

$$\bar{b}_n = -e^{\gamma_n}\left(1 + \lambda \frac{2e^{\gamma_{n+1}}}{\sinh\gamma_{n+1}\bar{Z}_{n+1}}\right)\bar{f}_n, \quad (5.29)$$

where

$$\bar{Z}_n = 1 + \lambda \frac{a_n^+ a_{n+1}^+}{\bar{Z}_{n+1}},$$

$$\bar{Z}_0 = 1 + \lambda \frac{a_0^- a_1^-}{\bar{Z}_1} + \lambda \frac{a_0^+ a_{-1}^+}{\bar{Z}_{-1}}. \quad (5.30)$$

We note that Eqs. (5.29) and (5.30) differ from Eqs. (5.27) and (5.28) by $\gamma_n \to -\gamma_n$ everywhere.

Equations for the scattering amplitudes with negative side band indices, $n < 0$, can be derived in a similar way, and the result differs from the above equations for positive side band indices [Eqs. (5.25)–(5.30)] by the substitution

$$\gamma_n \to -\gamma_{-|n|}, \quad n \neq 0, \quad (5.31)$$

which is introduced everywhere except in Z_0 and $\bar{Z}_0$

6. Quasiparticle current

In the nonstationary problem under consideration, the density matrix determining the current [Eq. (4.1)] is time dependent, and its dynamic evolution can be described by an equation similar to Eq. (4.3),

$$\langle \hat{\Psi}(\mathbf{r}, t)\, \hat{\Psi}^+(\mathbf{r}, t) \rangle = \sum_\lambda \Psi_\lambda(\mathbf{r}, t) f_\lambda \Psi_\lambda^+(\mathbf{r}, t), \quad (6.1)$$

Ψ_λ are now solutions of the time-dependent problem, Eq. (2.5), whose initial conditions correspond to the eigenstates of the initial Hamiltonian with the eigenvalues λ, and occupation numbers f_λ of these initial states. We consider the inelastic scattering states, [Eqs. (2.6) and (5.2)] as the propagators $\Psi_\lambda(t)$ in Eq. (6.1) with λ corresponding to the complete set of the incoming states $\lambda = (E, j)$; according to the assumption about local equilibrium within the electrodes, the incoming states possess the Fermi distribution of occupation numbers, $f_{Ej} = n_F(-E)$. Thus the current [Eq. (4.1)] takes the form

$$I(t) = -e \int_{|E|>\Delta} \frac{dE|E|}{2\pi\xi} n_F(-E) \sum_{N=-\infty}^{\infty} e^{iNeVt} \times$$

$$\times \sum_{n=-\infty}^{\infty} \sum_{j\beta} \beta(\psi_j^\beta(E, n), \psi_j^\beta(E, N+n)). \quad (6.2)$$

The current in Eq. (6.2) consists of a time-independent part, $N = 0$, which is formed by incoherent contributions from all the side bands (the quasiparticle current) and from a time-dependent part, $N \neq 0$, which results from interference among the different side bands (Josephson alternating current). The difference between the side band indices N is an even number since the side band index is either even or odd, depending on the electrode; therefore, the time-dependent current oscillates with the Josephson frequency $\omega = 2eV$.

In this paper we concentrate on an analysis of the time-independent quasiparticle current. By analogy with to Eq. (4.7), we calculate the current using the transmitted states,

$$I = \frac{1}{2}\frac{e}{\pi} \int_{|E|>\Delta} dE \frac{|E|}{\xi} n_F(-E) \times$$

$$\times \sum_{n=-\infty}^{\infty} \left[\sum_{j=1,3} (|f_{jn}|^2 - |b_{jn}|^2) + \sum_{j=2,4} (|a_{jn}|^2 - |c_{jn}|^2) \right]. \quad (6.3)$$

Using the scattering amplitudes introduced in the previous section through Eqs. (5.12), (5.14), (5.17), and (5.18), we express the current in Eq. (6.3) in the form

$$I = \frac{e}{\pi} \int_{|E|>\Delta} dE \frac{|E|}{\xi} n_F(-E) \sum_{\text{odd}} (K_n - \bar{K}_n), \quad (6.4)$$

where

$$K_n = \lambda^{|n|}\,(R^{-1}|f_n|^2 - |b_n|^2)\,,$$
$$\bar{K}_n = \lambda^{|n|}(R^{-1}|\bar{f}_n|^2 - |\bar{b}_n|^2) = K_n(-\gamma)\,. \qquad (6.5)$$

The factor of 2 appears in Eq. (6.4) because of equality of the currents I_1 and I_4 and the currents I_2 and I_3 in Eq. (4.8), which hold also in the nonstationary case. However, there is no balance between the currents of these two pairs any more. The symmetry of Eq. (5.20) allows us to reduce the interval of integration in Eq. (6.4) to the semiaxis $E > 0$,

$$I = \frac{e}{\pi}\int_{\Delta}^{\infty} dE\,\frac{E}{\xi}\tanh\frac{E}{2T}\sum_{\text{odd}}(K_n - \bar{K}_n)\,. \qquad (6.6)$$

The side band currents K_n in Eq. (6.5) are proportional to the powers of the small parameter λ, $K_n \sim \lambda^{|n|}$. Therefore, Eqs. (6.6) and (6.5) present a perturbative expansion of the current, which is convenient for analysis in the limit of low barrier transparency. In the following sections we carry out such an analysis of the structure of the current in Eq. (6.6).

7. Excess current at large bias

To make some useful observations for analysis of the subgap current, it is instructive first to discuss the simpler case of large bias $eV >> \Delta$, which has been studied extensively in literature [11,12,17,23]. We derive at the same time the explicit analytical expression for the current in this limit, which is valid in the whole range of the junction transparency, $0 < D < 1$. The asymptotic expansion of the current with respect to the small parameter Δ/eV has the form [17]

$$I = \frac{e^2 DV}{\pi} + I_{\text{exc}}(D) + O\left(\frac{\Delta}{eV}\right)\,, \qquad (7.1)$$

where the first term is the tunnel current of the normal junction and the second term is a voltage-independent excess current which represents the leading superconducting correction.

A main simplification in this case is that the side band currents K_n and $\bar{K}_n$, $|n| > 1$ diminish when the bias voltage increases. This follows from an estimate of the transmission amplitudes in Eqs. (5.27)–(5.29), which contain products of factors $|\sinh\gamma_k|^{-2}$ which are small at large voltages, $|\sinh\gamma_k|^{-2} \sim (\Delta/eV)^2$, because of the large interval of involved energies, $E \sim eV$. Furthermore, inspection of the amplitudes f_{-1} and $\bar{f}_1$ shows that they are also small due to the factors $\exp(-\gamma_0 - \gamma_1)$; therefore, the nonvanishing part of the current [Eq. (6.6)] in the limit $eV >> \Delta$ becomes

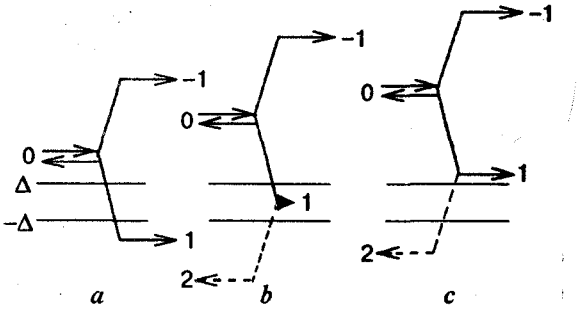

Fig. 6. Three kinds of processes that contribute to the tunnel current at large bias $eV >> \Delta$: creation of a real excitation across the gap by forward scattering (*a*); excitation of the Andreev bound state due to creation of a real excitation via backward scattering (dashed arrow) (*b*); imbalance of ground state modes due to creation of a real excitation via backward scattering (*c*). Excess current is caused by processes *b*) and c).

$$I = \frac{e}{\pi}\int_{\Delta}^{\infty} dE\,\frac{E}{\xi}\tanh\frac{E}{2T}\,(K_1 - \bar{K}_{-1})\,. \qquad (7.2)$$

The essential fragments of the scattering diagram in the large bias limit are shown in Fig. 6.

The structure of the current in Eq. (7.2) is essentially determined by the presence of a gap in the spectrum of the side band $n = 1$; this causes different analytical forms of the current K_1 in the regions $|E| < \Delta$ and $|E| > \Delta$. We note that the spectrum of the side band $n = -1$ possesses no gap: $E_{-1} > \Delta$ for $E > \Delta$. Accordingly, we divide the integral in Eq. (7.2) into three parts:

$$I = I_< + I_\Delta + I_>\,.$$

The first part corresponds to the current of the states in the side band $n = 1$, which lie below the gap, $E_1 < -\Delta$. The second part corresponds to the current of the states of the same side band which lie in the gap, $-\Delta < E_1 < \Delta$. The third part combines contributions from the remaining states of the side band $n = 1$, $\Delta < E_1$, and from all the states of the side band $n = -1$. Making use of the approximations

$$|Z_0|^2 = |\bar{Z}_0|^2 \approx |1 + 2\lambda(E+\xi)/\xi|^2\,,$$
$$|Z_{-1}|^2 = |\bar{Z}_1|^2 = |Z_2|^2 = |\bar{Z}_{-2}|^2 \approx 1\,, \qquad (7.3)$$
$$|Z_1|^2 = |\bar{Z}_{-1}|^2 = |Z_{-2}|^2 = |\bar{Z}_2|^2 \approx 1/R^2\,,$$

it is possible to express the integral $I_<$ in the form (we restrict the analysis to the limit $T = 0$):

$$I_< = \frac{e}{\pi}\int_{\Delta}^{eV-\Delta} dE\,\frac{E}{\xi}K_1 = \frac{8e\lambda}{\pi R}\int_{\Delta}^{eV/2} dE\,\frac{E}{\xi Z_0^2} - \frac{2e\lambda}{\pi R}\int_{\Delta}^{\infty} dE\,\frac{(E-\xi)}{\xi Z_0^2}\left(1 - 4\lambda R\,\frac{E}{\xi}\right), \quad (7.4)$$

where the limit of integration in the last term is extended to infinity since the main contribution to this integral comes from the energies $E \sim \Delta << eV$. Separating out the normal junction current, we can express Eq. (7.4) in the form

$$I_< = \frac{e^2 DV}{\pi} - \frac{8e\lambda^2}{\pi} \times \int_{\Delta}^{\infty} \frac{dE}{Z_0^2\xi}\left[4\lambda R\,\frac{E\Delta^2}{\xi^2} + (2R+1)\,\frac{E(E-\xi)}{\xi} + \frac{E-\xi}{4\lambda R}\right]. \quad (7.5)$$

We note that this current is always smaller than the normal current. It is convenient to express the integral I_Δ as

$$I_\Delta = \frac{e}{\pi}\int_{eV-\Delta}^{eV+\Delta} dE\,\frac{E}{\xi}K_1 = \frac{16e\lambda^2}{\pi}\int_0^{\Delta} dE\,\frac{\Delta^2}{|\xi Z_0|^2}, \quad (7.6)$$

which is found from the relations between the functions Z_n [which result from their definition in Eq. (5.25)]

$$Z_n(E+eV) = \bar{Z}_{n-1}(E),$$
$$Z_0(E+eV)Z_1(E+eV) = \bar{Z}_0(E)\bar{Z}_{-1}(E). \quad (7.7)$$

Inspection of the equation for $I_>$,

$$I_> = \frac{e}{\pi}\int_{eV+\Delta}^{\infty} dE\,\frac{E}{\xi}K_1 - \frac{e}{\pi}\int_{\Delta}^{\infty} dE\,\frac{E}{\xi}\bar{K}_{-1}, \quad (7.8)$$

shows that the two integrals diverge at the upper limit $E = \infty$, which means that the states lying far from the Fermi level formally contribute to the current, while the quasiclassical approximation of Eq. (2.6) assumes that all relevant states lie close to the Fermi level. To eliminate this formal divergence, the variable is commonly shifted by eV in the first integral in Eq. (7.8). Using again the relations (7.7) we express this integral in the form

$$\frac{4e\lambda}{\pi R}\int_{\Delta}^{\infty} dE\,\frac{E}{\xi Z_0 Z_{-1}} + \frac{8e\lambda^2}{\pi}\int_{\Delta}^{\infty} dE\,\frac{E(E-\xi)}{\xi^2 Z_0^2},$$

where the first term has the same analytical form but the opposite sign compared to the divergent term in the second integral in Eq. (7.8),

$$-\frac{4e\lambda}{\pi R}\int_{\Delta}^{\infty} dE\,\frac{E}{\xi Z_0 Z_{-1}} + \frac{2e\lambda}{\pi R}\int_{\Delta}^{\infty} dE\,\frac{(E-\xi)}{\xi Z_0^2}.$$

After elimination of the divergent terms, the integral in Eq. (7.8) takes the form

$$I_> = \frac{2e\lambda}{\pi R}\int_{\Delta}^{\infty} dE\,\frac{(E-\xi)}{\xi Z_0^2}\left(1 + 4\lambda R\,\frac{E}{\xi}\right). \quad (7.9)$$

The positive currents in Eq. (7.9) and Eq. (7.6) overcompensate the missing part of the current in Eq. (7.5). Collecting Eqs. (7.5), (7.6), and (7.9), we find after some algebra the following explicit equation for the excess current in Eq. (7.1):

$$I_{\rm exc} = \frac{16e\Delta\lambda^2 R}{\pi}\left[1 - \frac{D^2}{2(1+R)\sqrt{R}}\ln\frac{1+\sqrt{R}}{1-\sqrt{R}}\right], \quad (7.10)$$

which is valid in the whole interval of junction transparency $0 < D \le 1$. Asymptotics of this expression coincide with the results presented in literature [11,23], both in the limit of fully transparent ($D = 1$) constrictions, $I_{\rm exc} = 8e\Delta/3\pi$, and in the limit of low-transparency ($D << 1$) tunnel junctions, $I_{\rm exc} = e\Delta D^2/\pi$.

The above calculation reveals an important difference between the structure of the current in normal and superconducting junctions. In normal junctions, the current, e.g., in the right electrode (see Fig. 5,*c*) results from scattering states that lie above the local chemical potential, $E > \mu - eV$, while contribution from the energy interval $E < \mu - eV$ is equal to zero due to mutual cancellation of currents of the scattering states incident from the left and from the right (in Fig. 5,*a* the current-carrying energy region corresponds to negative energies, $E_h < 0$). Thus, the total current coincides with the current of real excitations emitted from the contact, which is consistent with the nonequilibrium origin of the current in the voltage-biased junctions. In superconducting junctions, only «across-the-gap» current $I_<$ is clearly related to the real excitations emitted at the right side of the junction where the current is calculated (Fig. 6,*a*): the dissipative character of the currents, I_Δ and $I_>$, is not

obvious. However, the creation of real excitations at the left side of the junction via backscattering into the side band $n = 2$ should be taken into account (Figs. 6,*b* and 6,*c*). Although the current of this side band exists only at the left side of the scattering diagram, it should have an effect at the right side due to continuity of the current at the interface [Eq. (4.5)] and therefore it should be distributed among the states of the side band $n = 1$. As our calculations show, this «kick» current partially flows through the Andreev bound states, which involve the current I_Δ (Fig. 6,*b*) and which convert this current into a supercurrent outside the junction. It is also partially distributed among the scattering states with positive energies (current $I_>$, Fig. 6,*c*) in the form of imbalanced ground state currents.

8. Subgap current

In this section we discuss the tunnel current in the subgap region, $eV < 2\Delta$. A basic property of the subgap current is the presence of temperature-independent structures on the I–V characteristics — the subharmonic gap structure (SGS). The SGS in tunnel junctions was discovered in experiments by Taylor and Burstein [56] and the first theoretical explanation was given by Schrieffer and Wilkins [42] in terms of multiparticle tunneling (MPT). Recently, the SGS has been observed in many experiments on transmissive tunnel junctions [3–5]. Although SGS in planar junctions can be attributed to normal shorts, the observation of SGS in superconducting controllable break junctions [8] provided convincing confirmation of the existence of SGS in the true tunnel regime.

The existence of SGS in tunnel current can be established within the MPT theory by means of rather simple perturbative arguments [42, 57–59]. Assuming a small perturbative coupling between electrodes, we can calculate, on the basis of the tunnel Hamiltonian model, the probability of tunneling in nth order of perturbation theory. Such a probability is proportional to a product of filling factors of the initial and the final states: $n_F(E)[1 - n_F(E - neV)]$. At zero temperature this factor is equal to zero outside the interval $\Delta < E < neV - \Delta$, which selects the quasiparticle transitions across the gap, i.e., the processes of creation of real excitations relevant for the tunnel current. Such a restriction places the threshold of the nth order current at $eV = 2\Delta/n$, and a sequence of current onsets of $\sim D^n$ at the voltages $eV = 2\Delta/n$ forms the SGS of the tunnel current [58, 59].

In our approach, the filling factors of final states do not enter the equation for the current Eq. (6.6), and the existence of SGS is therefore not obvious, although the side band currents [Eq. (6.5)] gradually decrease with increasing side band index. However, attribution of the nonequilibrium tunnel current in biased junctions to the current of real excitations is a general physical argument which should be automatically met in any correct theory. In fact, the true tunnel current, as we can see from the discussion of the previous section, is hidden in Eq. (6.6): it results from partial cancellation of large contribution of different scattering modes. The cancellation is nontrivial because of mixture of currents of different side bands, the odd side bands containing information about the currents of the even side bands and vice versa. This means that a finite perturbation expansion of Eq. (6.6) is not satisfactory and will not adequately correspond to the perturbative structure of the true tunnel current. To reveal such a structure one must rearrange the series in Eq. (6.6).

To this end, we consider a general term K_n , $n > 0$ in Eq. (6.6). It follows immediately from the explicit form of the normal and Andreev transmission coefficients [Eqs. (5.27) and (5.28)] that the leading term with respect to λ in K_n is proportional to a factor $[(1 - \exp(2\Gamma_n)]$, which is equal to zero if $|E_n| < \Delta$. Having made this observation, we express the quantity K_n in the form

$$K_n = \frac{2}{R}\lambda^n \theta(E_n^2 - \Delta^2)\, e^{-\gamma_n} \sinh\gamma_n |f_n|^2 + \\ + 4\lambda^{n+1} e^{-2\Gamma_n} \left|\frac{f_n}{Z_{n+1}}\right|^2 F_{n+1}, \qquad (8.1a)$$

$$F_{n+1} = |Z_{n+1}|^2 + \\ + \mathrm{Re}\left(\frac{e^{-\gamma_{n+1}} Z^*_{n+1}}{\sinh\gamma_{n+1}}\right) - \lambda\left|\frac{e^{-\gamma_{n+1}}}{\sinh\gamma_{n+1}}\right|^2. \qquad (8.1b)$$

In Eq. (8.1a) the first term represents the main contribution of the nth side band to the current: it is proportional to the probability of normal scattering to the nth side band and it does not contain the contribution of the side band states lying inside the gap $|E_n| < \Delta$. Using the recurrence relation (5.25) and recalling that $\lambda = D/4R$, after some algebra the function F_n in Eq. (8.1b) becomes

$$F_n = \frac{1}{R}\theta(E_n^2 - \Delta^2)\frac{1}{\tanh\gamma_n} - \lambda\left|\frac{e^{\gamma_n}}{\sinh\gamma_n Z_{n+1}}\right|^2 G_{n+1}, \qquad (8.2a)$$

$$G_{n+1} = |Z_{n+1}|^2 - \mathrm{Re}\left(\frac{e^{\gamma_{n+1}} Z^*_{n+1}}{\sinh \gamma_{n+1}}\right) - \lambda \left|\frac{e^{\gamma_{n+1}}}{\sinh \gamma_{n+1}}\right|^2 . \quad (8.2b)$$

Substituting Eq. (8.2) into Eq. (8.1a), we find that the second term in the equation for K_n, which is proportional to λ^{n+1}, has analytical structure similar to the first term in the same equation, proportional to λ^n, namely, it consists of the probability of normal scattering to the $(n+1)$th side band [cf. Eq. (5.22)] and it does not include the contribution of the side band states that lie inside the gap, $|E_{n+1}| < \Delta$. This allows us to associate this term with the effective contribution of the nearest *even* side band.

A similar transformation of the function G_{n+1} in Eq. (8.2) yields the recurrence relation

$$G_{n+1} = -\frac{1}{R}\theta(E^2_{n+1} - \Delta^2)\frac{1}{\tanh \gamma_{n+1}} - \lambda \left|\frac{\exp(-\gamma_{n+1})}{\sinh \gamma_{n+1} Z_{n+2}}\right|^2 F_{n+2} . \quad (8.3)$$

Combining of Eqs. (8.1a)–(8.3) shows that the next term of the current K_n, which is proportional to λ^{n+2}, has the same analytical structure as the leading term in the current K_{n+2} of the next odd side band, and therefore it can be regarded as a renormalization of that current.

Continuing this procedure by systematic use of the recurrence relations (8.2) and (8.3), we obtain the following expansion for the current K_n in Eq. (6.5):

$$K_n = \frac{2\lambda^n}{R}\theta(E^2_n - \Delta^2) Q_n + \frac{4\lambda^{n+1}}{R}\theta(E^2_{n+1} - \Delta^2) e^{-\Gamma_n} \cosh \Gamma_n Q_{n+1} + \frac{4\lambda^{n+2}}{R}\theta(E^2_{n+2} - \Delta^2) \times$$
$$\times \exp(-\Gamma_n + 2\Gamma_{n+1}) \cosh \Gamma_n Q_{n+2} + \frac{4\lambda^{n+3}}{R}\theta(E^2_{n+3} - \Delta^2) \exp(-\Gamma_n + 2\Gamma_{n+1} - 2\Gamma_{n+2}) \cosh \Gamma_n Q_{n+3} + \ldots , \quad (8.4)$$

where we have introduced the quantity Q_n defined for all n as

$$Q_n = \frac{e^{\gamma_0}}{\cosh \gamma_0 |Z_0|^2} \sinh \gamma_n \cosh \Gamma_n \prod_{l=1}^{n} \frac{1}{|Z_l \sinh \gamma_l|^2} . \quad (8.5)$$

Similar expansions can be derived for the currents $\bar{K}_n$ and for the currents of the side bands with negative $n < 0$. Expanding each term of the series in Eq. (6.6) with use of Eq. (8.4) and collecting the terms with the same factor λ^n, we can finally express the series in the form

$$\sum_{\text{odd}} (K_n - \bar{K}_n) = \sum_{n \neq 0} (\tilde{K}_n - \tilde{\bar{K}}_n) . \quad (8.6)$$

The last summation is done over all odd *and even* integer n, and the renormalized coefficients have the form

$$\tilde{K}_n = \lambda^n \theta(E^2_n - \Delta^2)(4Q_n/R)\left[(1/2) + \cosh \Gamma_{n-2} \exp(-\Gamma_{n-2} + 2\Gamma_{n-1}) + \right.$$
$$\left. + \cosh \Gamma_{n-4} \exp(-\Gamma_{n-4} + 2\Gamma_{n-3} - 2\Gamma_{n-2} + 2\Gamma_{n-1}) + \ldots + \cosh \Gamma_1 \exp(-\Gamma_1 + 2\Gamma_2 - 2\Gamma_3 + \ldots + 2\Gamma_{n-1})\right] \quad (8.7a)$$

for odd $n > 0$ and the form

$$\tilde{K}_n = \lambda^n \theta(E^2_n - \Delta^2)(4Q_n/R)\left[\cosh \Gamma_{n-1} e^{-\Gamma_{n-1}} + \right.$$
$$\left. + \cosh \Gamma_{n-3} \exp(-\Gamma_{n-3} + 2\Gamma_{n-2} - 2\Gamma_{n-1}) + \ldots + \cosh \Gamma_1 \exp(-\Gamma_1 + 2\Gamma_2 - 2\Gamma_3 + \ldots - 2\Gamma_{n-1})\right] \quad (8.7b)$$

for even $n > 0$.

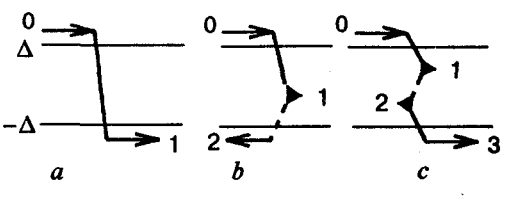

Fig. 7. Scattering processes that contribute to the subgap current: single-particle scattering into the side band $n = 1$ gives the main contribution at $eV > 2\Delta$ (*a*); excitation of the Andreev bound state ($n = 1$) due to backward scattering into the side band $n = 2$ gives the main contribution at $eV > \Delta$ (*b*); single-particle scattering into the side band $n = 3$ and simultaneous excitation of the Andreev bound state in the side band $n = 1$ gives the main contribution at $eV > 2\Delta/3$ (*c*).

The representation of Eqs. (8.6) and (8.7) is exact. A general term of the series can be regarded as an effective renormalized current of the nth side band. In fact, this effective current consists of the contributions of all side bands with odd indices smaller than n. An important feature of this representation is the presence of the θ-function in the general term, which allows us to separate out in Eq. (6.6) that part of the current which is obviously responsible for the SGS,

$$I_{SGS} = \sum_{n=1}^{\infty} \frac{e}{\pi} \int_{\Delta}^{neV-\Delta} dE \frac{E}{\xi} \tanh \frac{E}{2T} (\tilde{K}_n - \bar{\tilde{K}}_n). \quad (8.8)$$

One might expect (cf. Ref. 55) that Eq. (8.8) represents the subgap tunnel current at zero temperature and that the remaining part of the current in Eq. (6.6),

$$I_r = I - I_{SGS} = \sum_{n=1}^{\infty} \frac{e}{\pi} \left[\int_{neV+\Delta}^{\infty} dE \frac{E}{\xi} \tanh \frac{E}{2T} (\tilde{K}_n - \bar{\tilde{K}}_n) + \right.$$
$$\left. + \int_{\Delta}^{\infty} dE \frac{E}{\xi} \tanh \frac{E}{2T} (\tilde{K}_{-n} - \bar{\tilde{K}}_{-n}) \right], \quad (8.9)$$

corresponds to the current of thermal excitations. However, this separation is not exact. An analysis shows that the current in Eq. (8.9) does not vanish completely at $T = 0$, but contributes a small residual part. An important property of this residual current is that it does not contain any structureless component but demonstrates behavior similar to the current I_{SGS} in Eq. (8.8), thus resulting in a small correction to Eq. (8.8).

9. Subharmonic gap structure

The explicit analytical expressions (8.8) and (8.9) provide a basis for numerical calculation of the subgap current for small λ (low transparency) with any desirable accuracy. However, they are also convenient for qualitative discussion of the SGS. In this section we will analyze the SGS at zero temperature on the basis of Eq. (8.8).

The current–voltage characteristic $I_{SGS}(V)$ in Eq. (8.8) has a complex form consisting of a sum of renormalized side band currents $I_n(V, \lambda)$:

$$I_{SGS}(V, \lambda) = \sum_{n=1}^{\infty} I_n(V, \lambda),$$
$$I_n(V, \lambda) = \frac{e}{\pi} \int_{\Delta}^{neV-\Delta} dE \frac{E}{\xi} (\tilde{K}_n - \bar{\tilde{K}}_n). \quad (9.1)$$

The partial current-voltage characteristics $I_n(V, \lambda)$ are similar to each other, and it is convenient to analyze them independently.

According to Eq. (9.1) the partial current I_n starts with an onset at the threshold voltage $V_n = 2\Delta/en$. In the limit $\lambda \to 0$ the onset is infinitely sharp and its magnitude is

$$I_n(V_n, \lambda \to 0) = e \Delta D^n \frac{2n}{4^{2n-1}} \frac{n^{2n}}{(n!)^2}. \quad (9.2)$$

The jumps of the current at the thresholds result from the singular denominators in Eqs. (5.27) and (5.29), which are related to the singular density of states at the side band energy gap edges, $\sinh \gamma_k = 0$. Accumulation of these singularities in the high-order scattering amplitudes leads to a huge increase of the partial currents well above the corresponding thresholds — this causes the failure of multiparticle tunneling theory [57–59]. In our theory, the singularities are regularized by the factors

$$P_n = \prod_{k=0}^{n} |Z_k|^2 \quad (9.3)$$

in the denominators of the scattering amplitudes, Eq. (5.27). These factors are expressed in terms of the continued fractions Z_n [Eq. (5.25)], which therefore should be calculated with sufficient accuracy to preserve the singular parts of Z_n which provide regularization of the integrals.

The first-order current I_1 in Eq. (9.1) corresponds to direct one-particle scattering to the side band $n = 1$ (Fig 7,*a*). The explicit form of the current I_1 is

$$I_1 = \frac{2e\lambda}{\pi R} \int_{\Delta}^{eV-\Delta} dE \frac{|E_1|}{\xi \xi_1} \left(\frac{E + \xi}{P_1} + \frac{E - \xi}{\bar{P}_1} \right). \quad (9.4)$$

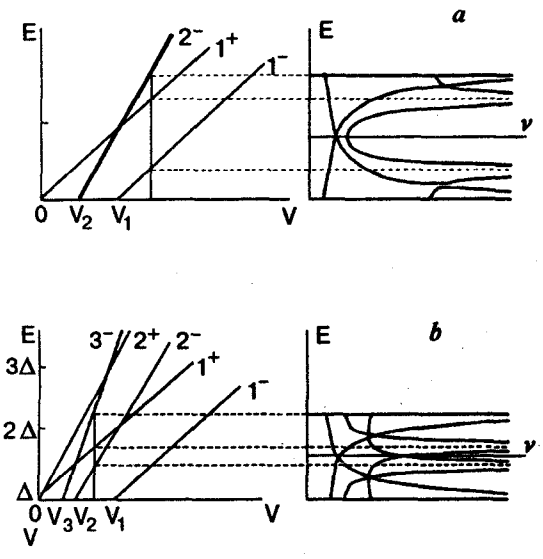

Fig. 8. a) Density of states $\nu(E) = |E_n/\xi_n|$ of the side bands and E_0, E_1, and E_2 at applied voltage $V > V_1$ (right), position of singularities of the side-band density of states plotted as function of the applied voltage for the current I_2 (left), $1^{\pm}: E_1 = \pm\Delta$, $2^{-}: E_2 = -\Delta$. *b)* Density of states of the side bands E_0, E_1, E_2, and E_3 at applied voltage $V_2 < V < V_1$ (right), position of singularities of the side-band density of states plotted as a function of the applied voltage for the current I_3 (left), $1^{\pm}: E_1 = \pm\Delta, 2^{\pm}: E_2 = \pm\Delta, 3^{-}: E_3 = -\Delta$.

In the limit $\lambda \to 0$ this current coincides with the quasiparticle current of the tunnel Hamiltonian model [54,60]. At finite λ the threshold onset of the current at $V = V_1$ is washed out. To evaluate the width of the onset we truncate the continued fraction in P_1 assuming $Z_{-1} = Z_2 = 1$, which yields

$$P_1 \approx \left| (1 + \lambda a_0^- a_{-1}^-)(1 + \lambda a_1^- a_2^-) + \lambda a_0^+ a_1^+ \right|^2 . \quad (9.5)$$

The function $\overline{P}_1$ has a similar form. The regularization effect of the threshold singularity is provided by the most singular term $\lambda a_0^+ a_1^+$ in Eq. (9.5). Keeping this term, we obtain in the vicinity of the threshold, $e(V - V_1) \ll \Delta$, the result

$$I_1(V) = \frac{2e\Delta\lambda}{\pi R} f\left(\frac{eV - eV_1}{\Delta\lambda}\right), \qquad f(z) = \int_0^{\pi} d\theta \frac{\sin^2\theta}{(\sin\theta + 1/z)^2} . \quad (9.6)$$

According to this formula the onset width is $e(V - V_1) \sim \lambda\Delta$.

The second-order current I_2 corresponds to the creation of a real excitation during quasiparticle backscattering into the side band $n = 2$ (Fig. 7,*b*) and appears as the current of transmitted states of the side band $n = 1$ (cf. the excess current in Sec. 7). In the vicinity of the threshold, $V_2 < V < V_1$, this current exists only in the form of currents through the bound states and therefore it is completely converted into a supercurrent far away from the junction. At larger voltages, $V > V_1$, the side band $n = 1$ extends outside the energy gap (see Fig. 8,*a*), which also makes the current I_2 partially consist of contributions from extended states. The explicit expression for the second-order current is

$$I_2 = \frac{4e\Delta^3\lambda^2}{\pi R} \int_{\Delta}^{2eV-\Delta} dE \frac{|E_2|}{\xi\xi_2|\xi_1|^2} \times \cosh\Gamma_1 \left(\frac{e^{-\gamma_0 + \Gamma_1}}{P_2} + \frac{e^{\gamma_0 - \Gamma_1}}{\overline{P}_2} \right) . \quad (9.7)$$

Omitting the λ-dependence of P_2 in Eq. (9.7), we obtain the two-particle tunnel current of Schrieffer and Wilkins [42,57]. To keep the singular terms in P_2 one has to truncate the continued fractions in Eq. (5.25) assuming $Z_{-1} = Z_3 = 1$, which yields

$$P_2 \approx \left| (1 + \lambda a_{-1}^- a_0^-) \times (1 + \lambda a_1^- a_2^-) + \lambda a_0^+ a_1^+ (1 + \lambda a_2^+ a_3^+) \right|^2 . \quad (9.8)$$

The threshold singularity results from the small product $\xi\xi_2$ in the denominator of Eq. (9.7). However, in Eq. (9.8) there are no singular terms proportional to $a_0 a_2$ among the terms linear in λ. Such terms are quadratic in λ and they provide, along with the terms λa_0 and λa_2, the width of the onset: $e(V - V_2) \sim \lambda^2\Delta$. This onset is sharper than the onset of the current I_1.

The threshold singularity in the current I_2 is typical of all higher-order currents $n > 1$. The appearance of the first side band outside the energy gap at $V = V_1$ is manifested through a spike in the current I_2. Indeed, if $V \approx V_1$, the nodes of ξ_1 overlap the nodes of ξ and ξ_2 at the lower ($E = \Delta$) and the upper ($E = 3\Delta$) limits of integration in Eq. (9.7), respectively (see Fig. 8,*a*). This singularity yields an increase of the current I_2 when the voltage approaches V_1,

$$I_2 \sim e\Delta\lambda^2 \left(\frac{\Delta}{e(V_1 - V)} \right)^{1/2} .$$

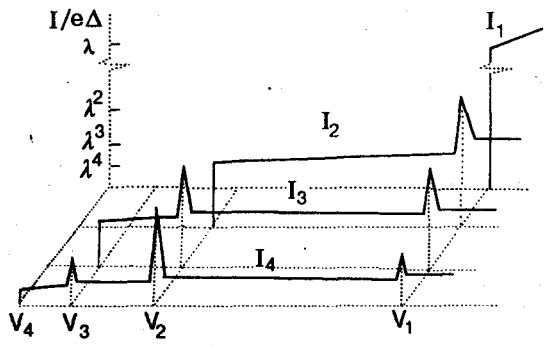

Fig. 9. Schematic diagram of the partial I_n–V characterstics.

Regularization of the integral, which is provided by the singular terms $\lambda a_1 a_0$ and $\lambda a_1 a_2$ in Eq. (9.8) at the lower and the upper integration limits, respectively, yields

$$\frac{I_2(V_1)}{I_2(V_2)} \sim \frac{1}{\sqrt{\lambda}}.$$

Further analysis shows that the current reaches a maximum value slightly above $V = V_1$, after which it rapidly decreases (see Fig. 9). At voltages $V > V_1$ the singular point $\xi_1 = 0$ remains within the integration region, which increases the current by a logarithmic factor in comparison with the value of the current near the threshold V_2,

$$I_2(V > V_1) \sim \frac{e\Delta\lambda^2 \ln\lambda}{R}. \qquad (9.9)$$

At large voltage $V >> V_1$ the current I_2 forms the excess current [Eq. (7.10)]. It is interesting to note that in this limit the logarithmic factor is compensated for by the current I_r [Eq. (8.9)], which yields the λ^2-dependence of the excess current.

The third-order current I_3 at voltages close to the threshold V_3 results from the combination of one-particle tunneling into the side band $n = 3$ and excitation of the transmitted Andreev bound states of the side band $n = 1$ (Fig. 7,*c*). The probabilities of these two processes are related as 1:2 at threshold [Eq. (8.7)]. A gradual emergence of the bound states of the side bands $n = 1$ and 2 outside the energy gap at $V = V_2$ and $V = V_1$ (Fig. 8,*b*) gives rise to the current peaks. The current I_3 has the explicit form:

$$I_3 = \frac{2e\Delta^5\lambda^3}{\pi R}\int_{\Delta}^{3eV-\Delta} dE \frac{|E_3|}{\xi\xi_3|\xi_1\xi_2|^2}\left[\frac{e^{\gamma_0}(1 + 2\cosh\Gamma_1 e^{-\Gamma_1+2\Gamma_2})}{P_3} + \frac{e^{-\gamma_0}(1 + 2\cosh\Gamma_1 e^{\Gamma_1-2\Gamma_2})}{\bar{P}_3}\right] \qquad (9.10)$$

with the regularization factor

$$P_3 \approx \left|(1 + \lambda a_{-1}^- a_0^-)(1 + \lambda a_1^- a_2^-)(1 + \lambda a_3^- a_4^-) + \lambda a_0^+ a_1^+ (1 + \lambda a_2^+ a_3^+)\right|^2. \qquad (9.11)$$

The current peak at $V = V_2$ results from the overlap of nodes of ξ and ξ_2 at $E = \Delta$ and nodes of ξ_1 and ξ_3 at $E = 2\Delta$, similarly to the peak of the current I_2. These singularities yield again an increase in the current inversely proportional to the square root of the departure from the voltage V_2: $I_3 \sim e\Delta^{3/2}\lambda^3/[e(V_2 - V)]^{1/2}$. However, since the factor P_3 [Eq. (9.11)] contains neither the term $\lambda a_0 a_2$ nor the term $\lambda a_1 a_3$, regularization of the singularity is provided, e.g., at $E = \Delta$, by the terms λa_0 or λa_2, which gives rise to a more pronounced peak with magnitude

$$\frac{I_3(V_2)}{I_3(V_3)} \sim \frac{1}{\lambda}. \qquad (9.12)$$

We note that the magnitude of this peak is comparable to the magnitude of the onset of the current I_2. The second peak at $V = V_1$ results from the overlap of the nodes of ξ_2 and ξ_3 at $E = 3\Delta$, which increases the current I_3 near the voltage $V = V_1$ which is inversely proportional to the first power of the distance to this voltage: $I_3 \sim \lambda^3\Delta^2/(V_1 - V)$. The divergence is regularized by the term $\lambda a_2 a_3$ in Eq. (9.11), which results in a peak of magnitude

$$\frac{I_3(V_1)}{I_3(V_3)} \sim \frac{1}{\lambda}. \qquad (9.13)$$

Thus the heights of the two peaks of the current I_3 are of the same order in λ, although the peak at $V \approx V_1$ is sharper.

In a similar way, all of the high-order currents in the vicinity of their thresholds are attributable either to the Andreev bound state currents (even n) or to a combination of Andreev bound state currents and the current of a single real excitation (odd n). The number of excited Andreev states is correspondingly $n/2$ or $(n-1)/2$. Singularities similar to the singularity of the current I_3 at the voltage $V \approx V_1$ exist in all high-order currents, where they cause even more pronounced current peaks because of the absence of terms $\lambda a_k a_{k+1}$ in the corresponding smearing functions P_n. Besause of this property, the heights of such peaks exceed the threshold value of the corresponding current by two orders of λ: $(I_n)_{\max} \sim e\Delta\lambda^{n-2}/R$.

The above discussion reveals the current peaks to be essential features of the SGS of tunnel current in addition to the current onsets (Fig. 9) (these peaks are seen also in the numerical results of Refs. 34 and 39). It allows us to establish a general classification of singularities that cause peaks in partial currents I_n. They result from the overlap of singularities of the side band density of states. It is easy to see that the singularities of only two side bands can overlap. The condition of the overlap for mth and kth side bands have the form

$$E - keV = \Delta, \quad E - meV = -\Delta. \qquad (9.14)$$

This condition is met at voltages $eV = 2\Delta/(m-k)$ for all integer $0 \le k < m \le n$. The magnitude of the current peaks depends on whether the overlapping side bands are neigbors or not, and whether the side band index is inside or at the edge of the interval $(0, n)$.

I. $m - k = 1$, $m = n$ or $k = 0$: edge-type singularity, neighbor side bands. This type of singularity forms the peak of the current I_2 at the main threshold V_1. The magnitude of the current peak is $(I_2)_{\max} \sim e\Delta\sqrt{\lambda}/R$.

II. $m - k > 1$, $m = n$ or $k = 0$: edge-type singularity, non-neighbor side bands. This type of singularity forms the first peak of each current I_n, $n > 2$ at voltage V_{n-1}. The magnitude of the current peak is $(I_n)_{\max} \sim e\Delta\lambda^{n-1}/R$.

III. $m - k = 1$, $m < n$, $k > 0$: internal singularity, neighbor side bands. This type of singularity forms the last peak of each current I_n, $n > 2$ at voltage V_1. The magnitude of the current peak is $(I_n)_{\max} \sim e\Delta\lambda^{n-1}/R$.

IV. $m - k > 1$, $m < n$, $k > 0$: internal singularity, non-neighbor side bands. This type of singularity forms all intermediate peaks of each current I_n, $n > 3$. The magnitude of the current peaks are $(I_n)_{\max} \sim e\Delta\lambda^{n-2}/R$.

Conclusion

In this paper we have considered superconductive tunneling as a scattering problem within the framework of Bogolyubov-de Gennes (BdG) quantum mechanics. An essential aspect of this problem is that the scatterer consists not only of the potential of the tunnel barrier but also of the discontinuity of the phase of the order parameter. At equilibrium (zero bias, Josephson direct current) the scattering problem is *elastic*. The peculiar feature of the elastic scattering problem in short junctions, which is considered here, is that the balance of currents of the scattering modes is not violated: the supercurrent flows only through the superconducting bound states (for a more general discussion, see Ref. 48). In the presence of voltage bias the scattering is *inelastic*, because the time dependence of the component of the scatterer is related to the superconducting phase difference. In general, the currents of all inelastic channels, taken collectively, constitute the components of the tunnel current that flows through the biased junction. The quasiparticle current corresponds to the incoherent part of the inelastic side band contributions, and the Josephson alternating current corresponds to the interference of the side band contributions.

There are three distinct components of the quasiparticle tunnel current at zero temperature: (i) the current of quasi-particles excited above the ground state, (ii) the current trough Andreev bound states converted to a supercurrent outside the junction, and (iii) the imbalance current of the ground state modes. At large bias voltage, $eV >> 2\Delta$, the first component corresponds to a single particle current of the normal junction, while the other components cause excess current. When voltage is decreased, redistribution of current among the components gives rise to subharmonic gap structure (SGS) in the form of current onsets and current peaks. Within the voltage intervals $2\Delta/n < eV < 2\Delta/(n-1)$ with even n, the tunnel current consists entirely of currents through the Andreev bound states [component (ii); e.g., Fig. 7,*b*]; the states of all side bands with odd indices smaller than n contribute to the current. If n is odd, a real excitation current of the side band n [component (i); e.g., Figs. 7,*a*, and 7,*c*] is also present in the tunnel current. Opening of new channels of tunneling of real excitations gives rise to current structures. Thus, SGS reveals the discrete nature of the side band spectrum. The structure becomes more

pronounced with decreasing transparency of the junction.

Since each Andreev state provides transfer of one Cooper pair through the junction for every incident quasi-particle, n particles will tunnel in the interval $2\Delta/n < eV < 2\Delta/(n-1)$.

The participation of a large number of bound Andreev states in the current transport at low voltages is surprising: it appears to contradict the fact that subgap current diminishes at zero bias. After all, the probability of the scattering into side bands does not depend on the bias and is proportional to powers of D. This paradox can be solved by increasing the compensation of currents between the normal and Andreev channels in each side band with decreasing voltage, which gives the required voltage dependence of the total current.

Acknowledgement

This work was supported by the Swedish National Science Research Council (NFR), the Swedish National Board for Technical and Industrial Development (NUTEK), and the Swedish Royal Academy of Sciences (KVA).

Appendix A: Boundary conditions

The quasiclassical boundary condition in Eqs.(2.8) and (2.9) has been derived in Ref. 31 by using the method of Ref. 21. Here we present simple arguments which lead to this boundary condition. We consider the more general case of asymmetric junction, using an asymmetric version of the Hamiltonian of Eq. (2.2) with the same restriction imposed on the length of the nonsuperconducting region, $L \ll \xi_0$. We include a contact potential difference in the potential $U(x)$, which implies that this potential may have nonvanishing asymptotic values at infinity: $U(-\infty) \neq U(\infty) \neq 0$. If the junction has more than one transverse transport mode, we assume that these modes are not mixed.

A one-dimensional quasiclassical wave function of a given transverse channel in the right electrode has the form [Eq.(2.6)],

$$\Psi_R(x,t) = \sum_\beta \frac{1}{\sqrt{v_R}} \times$$

$$\times \exp\left(i\beta \int p_R dx\right) \exp\left(i\sigma_z \chi_R/2\right) \psi_R^\beta(x,t)\,, \quad \text{(A.1)}$$

with a similar expression for the left electrode. The quantities ψ_R^β are slowly varying two-component wave functions on the scale of $1/p_R$, where $p_R(x) = [2m_R(\mu - U_R - E_{\perp R}(x))]^{1/2}$. This equation is valid over the distance $x \gg 1/p_R$ from the junction, and in the spatial region $1/p_R \ll x \ll \xi_0$ the functions ψ_R^β are almost constant.

From another point of view, at large distance from the junction, $|x| \gg 1/p_{R,L}$, the function Ψ can be expressed in the form of a linear combination of the scattering states at the Fermi level,

$$\Psi = C_1\chi_1 + C_2\chi_2 \quad \text{(A.2)}$$

$$\chi_1 = \begin{cases} (1/\sqrt{v_L})\left[e^{ip_L x} + re^{-ip_L x}\right], & x<0\,, \\ (1/\sqrt{v_R})\,d\,e^{ip_R x}, & x>0\,, \end{cases} \quad \text{(A.3a)}$$

$$\chi_2 = \begin{cases} 1/\sqrt{v_R}\left[e^{-ip_L x} + \tilde{r}e^{-ip_R x}\right], & x>0\,, \\ (1/\sqrt{v_L}\,\tilde{d}\,e^{-ip_L x}, & x<0\,, \end{cases} \quad \text{(A.3b)}$$

Comparing Eqs. (A.2) and (A.3) with Eq. (A.1) in the region $1/p_F \ll |x| \ll \xi_0$, we have

$$C_1 = e^{i\sigma_z \chi_L/2}\psi_L^+\,,\ C_2 = e^{i\sigma_z \chi_R/2}\psi_R^-\,,$$
$$rC_1 + \tilde{d}C_2 = e^{i\sigma_z \chi_L/2}\psi_L^-\,, \quad \text{(A.4)}$$
$$dC_1 + \tilde{r}C_2 = e^{i\sigma_z \chi_R/2}\psi_R^+\,,$$

which yields the boundary condition

$$\begin{pmatrix}\psi^- \\ \psi^+\end{pmatrix} = \hat{V}\begin{pmatrix}\psi^+ \\ \psi^-\end{pmatrix}, \quad \text{(A.5)}$$

with the matching matrix

$$\hat{V} = \begin{pmatrix} r & \tilde{d}\,e^{i\sigma_z\varphi/2} \\ d\,e^{-i\sigma_z\varphi/2} & \tilde{r} \end{pmatrix}, \quad \text{(A.6)}$$

where $\varphi = \chi_R(0) - \chi_L(0)$. The matrix $\hat{V}$ satisfies the unitarity condition $\hat{V}\hat{V}^+ = 1$, provided by the relations among the normal electron scattering amplitudes in Eq. (A.3): $\tilde{r} = -\tilde{d}(r/d)^*$, $|d|^2 = |\tilde{d}|^2 = D$, $|r|^2 = |\tilde{r}|^2 = R = 1 - D$.

Appendix B: Bound state current

Equation (4.10) for the current of a single bound state can be derived directly [61] from the Bogolyubov-de Gennes equations (2.5) and (2.2). The derivation is valid for junctions with an arbitrary nonsuperconducting region between the superconducting electrodes. We assume for simplicity that the phase of the order parameter [Eq.(2.3)] in the electrodes is constant and equal to $\pm\varphi/2$ in the right and left

electrodes, respectively. Let $\Psi(\mathrm{r}, E)$ be a normalized wave function of the Andreev bound state with energy E,

$$\hat{H}\Psi - E\Psi = 0\,,\ \Psi(x = \pm\infty) = 0\,. \qquad \text{(B.1)}$$

The energy and the wave function of the bound state depend on the phase difference φ. Using the derivative with respect to φ in Eq. (B.1) and a scalar product of the resulting equation with the function Ψ, we obtain

$$\int d^3 r\left(\Psi, \frac{d}{d\varphi}(\hat{H} - E)\Psi\right) = 0\,, \qquad \text{(B.2)}$$

where the brackets denote a scalar product in the electron-hole space, similar to Eq. (3.8). In this equation the derivative of the Hamiltonian has the form

$$\frac{d\hat{H}}{d\varphi} = \frac{d\hat{\Delta}}{d\varphi} = \frac{i\,\mathrm{sign}\,x}{2}\sigma_z\hat{\Delta}\,, \qquad \text{(B.3)}$$

in accordance with Eqs. (2.2) and (2.3). Substituting relation (B.3) into Eq. (B.2) and taking into account that the function Ψ is normalized, we obtain

$$\frac{dE}{d\varphi} = \int d^3 r\left(\Psi, \frac{d\hat{\Delta}}{d\varphi}\Psi\right). \qquad \text{(B.4)}$$

The continuity equation for the charge current,

$$I(x, E) = \frac{e}{2m}(\hat{p}_x - \hat{p}'_x)\int d^2 r_\perp \langle\Psi(x'), \Psi(x)\rangle_{x=x'}\,, \qquad \text{(B.5)}$$

in accordance with Eq. (B.1), has the form

$$i\frac{d}{dx}I(x, E) = e\int d^2 r_\perp\left(\Psi(x), [\sigma_z, \hat{\Delta}]\Psi(x)\right). \qquad \text{(B.6)}$$

Substituting relation (B.3) into Eq. (B.6) and integrating this equation over the entire x axis, we obtain

$$I(0,E) = 2e\int d^3 r\left(\Psi, \frac{d\hat{\Delta}}{d\varphi}\Psi\right). \qquad \text{(B.7)}$$

In Eq. (B.7) the current at infinity drops out because of decay of the bound state wave function, $I(\pm\infty) = 0$. The current $I(0)$ is formally taken in the middle of the junction; however, the current has the same value in the whole nonsuperconducting region, according to the conservation equation (B.6). Comparison of Eqs. (B.4) and (B.7) finally yields

$$I(E) = 2e\frac{dE}{d\varphi}\,. \qquad \text{(B.8)}$$

1. J. Bardeen, *Phys. Rev. Lett.* **6**, 57 (1961).
2. A. Barone and G. Paterno, *Physics and Applications of the Josephson Effect*, Wiley, New York (1982).
3. C. L. Foden, R. Rando, A. van Dordrecht, A. Peacock, J. Lumley, and C. Pereira, *Phys. Rev.* **B47**, 3316 (1993).
4. R. Cristiano, I. Franzio, R. Monaco, C. Nappi, and S. Pagano, *Phys. Rev.* **B49**, 429 (1994).
5. A. W. Kleinsasser, R. E. Miller, W. H. Mallison, and G. B. Arnold, *Phys. Rev. Lett.* **72**, 1738 (1994).
6. H. Takayanagi and T. Kawakami, *Phys. Rev. Lett.* **54**, 2449 (1985).
7. A. Frydman and Z. Ovadyahu, *Solid State Commun.* **95**, 79 (1995).
8. N. van der Post, E. T. Peters, I. K. Yanson, and J. M. van Ruitenbeek, *Phys. Rev. Lett.* **73**, 2611 (1994).
9. H. Takayanagi, T. Akazaki, and J. Nitta, *Phys. Rev. Lett.* **75**, 3533 (1995).
10. W. Haberkorn, H. Knauer, and J. Richter, *Phys. Status Solidi* **47**, K161 (1978).
11. A. V. Zaitsev, Zh. *Eksp. Teor. Fiz.* **86**, 1742 (1983) [*Sov. Phys. JETP* **59**, 1015 (1984)].
12. G. B. Arnold, *J. Low Temp. Phys.* **59**, 143 (1985).
13. L. G. Aslamasov and B. Fistul', *Zh. Eksp. Teor. Fiz.* **83**, 1170 (1982) [*Sov. Phys. JETP* **56**, 666 (1982)].
14. C. Ishii, *Prog. Theor. Phys.* **44**, 1525 (1970).
15. A. V. Svidzinsky, T. N. Anzygina, and E. N. Bratus', *J. Low Temp. Phys.* **10**, 131 (1973).
16. I. O. Kulik and A. N. Omel'yanchuk, *Fiz. Nisk. Temp.* **3**, 945 (1977); 4 , 296 (1978) [*Sov. J. Low Temp. Phys.* **3**, 459 (1977); 4, 142 (1978)].
17. S. N. Artemenko, A. F. Volkov, and A. V. Zaitsev, *Zh. Eksp. Teor. Fiz.* **76**, 1816 (1979) [*Sov. Phys. JETP* **49**, 924 (1979)].
18. I. O. Kulik, *Zh. Eksp. Teor. Fiz.* **57**, 1745 (1969) [*Sov. Phys. JETP* **30**, 944 (1970)].
19. J. Bardeen and J. L. Jonson, *Phys. Rev.* **B5**, 72 (1972).
20. P. G. de Gennes, *Superconductivity of Metals and Alloys*, Addison-Wesley, New York (1989).
21. A. V. Svidzinsky, *Spatial Inhomogeneity Problems in the Theory of Superconductivity*, Nauka, Moscow (1982) (in Russian).
22. I. F. Itskovich and R. I. Shekhter, *Fiz. Nizk. Temp.* **7**, 863 (1981) [*Sov. J. Low Temp. Phys.* **7**, 418 (1981)].
23. G. E. Blonder, T. M. Klapwijk, and M. Tinkham, *Phys. Rev.* **B25**, 4515 (1982).
24. C. W. J. Beenakker and H. van Houten, *Phys. Rev. Lett.* **66**, 3056 (1991).
25. P. F. Bagwell, *Phys. Rev.* **B46**, 12573 (1992).
26. C. W. J. Beenakker, *Phys. Rev. Lett.* **67**, 3836 (1991).
27. M. Hurd and G. Wendin, *Phys. Rev.* **B49**, 15258 (1994).
28. L. Y. Gorelik, V. S. Shumeiko, R. I. Shekhter, G. Wendin, and M. Jonson, *Phys. Rev. Lett.* **75**, 1162 (1995).
29. A. Furusaki and M. Tsukada, *Physica* **B165–166**, 967 (1990); *Phys. Rev.* **B43**, 10164 (1991).
30. C. W. J. Beenakker and H. van Houten, in: *Single Electron Tunneling and Mesoscopic Devices*, Springer, Berlin (1991).
31. V. S. Shumeiko, E. N. Bratus', and G. Wendin, *Phys. Rev.* **B48**, 13129 (1993).
32. T. M. Klapwijk, G. E. Blonder, and M. Tinkham, *Physica* **B+C 109–110**, 1657 (1982).
33. E. N. Bratus', V. S. Shumeiko, and G. Wendin, *Phys. Rev. Lett.* **74**, 2110 (1995).
34. D. Averin and A. Bardas, *Phys. Rev. Lett.* **75**, 1831 (1995).
35. B. J. van Wees, H. van Houten, C. W. J. Beenakker, J. G. Williamson, L. P. Kouwenhoven, D. van der Marel, and C. T. Foxon, *Phys. Rev. Lett.* **60**, 848 (1988).
36. R. Landauer, *IBM J. Res. Dev.* **1**, 223 (1957).
37. S. V. Kuplevakhskii and I. I. Fal'ko, *Fiz. Nizk. Temp.* **17**, 961 (1991) [*Sov. J. Low Temp. Phys.* **17**, 501 (1991)].
38. B. D. Josephson, *Adv. Phys.* **14**, 419 (1965).
39. G. B. Arnold, *J. Low Temp. Phys.* **68**, 1 (1987).
40. A. D. Stone, M. Ya. Azbel, and P. A. Lee, *Phys. Rev.* **B31**, 1707 (1985).
41. P. F. Bagwell and R. K. Lake, *Phys. Rev.* **B46**, 15329 (1992).
42. J. R. Schrieffer and J. W. Wilkins, *Phys. Rev. Lett.* **10**, 17 (1963).
43. L. I. Glazman, G. B. Lesovik, D. E. Khmel'nitskii, and R. I. Shekhter, *Pis'ma Zh. Eksp. Teor. Fiz.* **48**, 218 (1988) [*JETP Lett.* **48**, 238 (1988)].

44. J. Bardeen, R. Kümmel, A. E. Jacobs, and L. Tewordt, *Phys. Rev.* **187**, 556 (1969).
45. I. O. Kulik, R. I. Shekhter, and A. N. Omel'yanchouk, *Solid State Commun.* **23**, 301 (1977).
46. M. Yu. Kupriyanov and V. F. Lukichev, *Zh. Eksp. Teor. Fiz.* **94**, 139 (1988) [*Sov. Phys. JETP* **67**, 1163 (1988)].
47. I. A. Devyatov and M. Yu. Kupriyanov, *Pis'ma Zh. Eksp. Teor. Fiz.* **59**, 187 (1994) [*JETP Lett.* **59**, 200 (1994)].
48. G. Wendin and V. S. Shumeiko, *Phys. Rev.* B53, R6006 (1996).
49. A. F. Andreev, *Zh. Eksp. Teor. Fiz.* **46**, 1823 (1964) [*Sov. Phys. JETP* **19**, 1228 (1964)].
50. J. R. Schrieffer, *Theory of Superconductivity*, Benjamin, New York (1964).
51. V. P. Galaiko, *Zh. Eksp. Teor. Fiz.* **61**, 382 (1971) [*Sov. Phys. JETP* **34**, 203 (1972)].
52. The contribution from the continuum does not vanish if there is imbalance of populations of electron-like and hole-like branches of the quasiparticle spectrum in one of the electrodes.
53. V. Ambegaokar and A. Baratoff, *Phys. Rev. Lett.* **10**, 468 (1963).
54. N. R. Werthamer, *Phys. Rev.* **147**, 255 (1966).
55. E. N. Bratus' and V. S. Shumeiko, *Fiz. Tverd. Tela* **21**, 2821 (1979) [*Sov. Phys. Solid State* **21**, 1506 (1979)].
56. B.N. Taylor and E. Burstein, *Phys. Rev. Lett.* **10**, 14 (1963).
57. J. W. Wilkins, in: *Tunneling Phenomena in Solids*, Plenum, New York (1963).
58. L. E. Hasselberg, *J. Phys.* F3, 1438 (1973); L. E. Hasselberg, M. T. Levinsen, and M. R. Samuelsen, *Phys. Rev.* B9 3757 (1974).
59. E. L. Wolf, *Principles of Electron Tunnel Spectroscopy*, Oxford University, New York (1985).
60. M. H. Cohen, L. H. Falicov, and J. C. Phillips, *Phys. Rev. Lett.* 8, 316 (1962).
61. L. Y. Gorelik, *unpublished*.